AALTO UNIVERSITY
School of Engineering
Department of Applied Mechanics

Irina Filatova

Analysis of nozzle flexibility in nozzle-vessel intersection in piping system

Thesis submitted in partial fulfillment of the requirements for the degree of
Master of Science in Technology

Espoo, August 8, 2013

Supervisor: Professor Gary Marquis

Instructors: Matti Tapio Hämäläinen, MSc (Tech.); Rikumatti Paldanius, BSc (Tech.); Sergei Lemetti, BSc (Tech.)

Aalto University
School of Engineering

Aalto University, P.O. BOX 11000, 00076 AALTO
www.aalto.fi

Abstract of master's thesis

Author: Irina Filatova

Title of thesis: Analysis of nozzle flexibility in nozzle-vessel intersection in piping system

Degree programme: Master's programme in Mechanical Engineering

Major/minor: Mechanics of Materials | Code of professorship: Kul-49

Thesis supervisor: Professor Gary Marquis

Thesis advisors: Matti Tapio Hämäläinen, MSc (Tech.); Rikumatti Paldanius, BSc (Tech.); Sergei Lemetti, BSc (Tech.)

Date: 08.08.2013 | Number of pages: 61+40 | Language: English

Abstract:

The goal of the work is to research the flexibility of the nozzle-vessel connection in pipeline system. In conventional methods of piping stress analysis nozzle-vessel juncture is assumed to be rigid. In reality, the juncture possesses the flexibility. Ignoring the nozzle flexibility in stress analysis leads to large overvaluation of the nozzle loads.

State of art had been studied and evaluated. Modern state of research of nozzle flexibility had been performed primarily for the vessels not subjected to pressure.

In this work comparison of different methods of flexibility calculation had been prepared. Existing piping system had been created and simulated in finite element method software. In code-based software most conservative assumption with vessel-nozzle junction and flanges fixed; with nozzle flexibility had been simulated. Finite element method model had been built and simulated with maximum flexible nozzles and another finite element method model with flange connection fixed. After comparison of the results had been established that the FEM model of the system with nozzle-vessel junction free to move possesses highest flexibility with lowest nozzle reactions. Highest reactions had been obtained for the system with fixed nozzles and flanges. The results of work give the suggestion of utilizing the nozzle flexibilities in piping stress analysis in order to achieve higher accuracy of results.

Keywords: piping stress analysis, nozzle flexibility, nozzle stiffness

Acknowledgements

This thesis had been written in and funded by Neste Jacobs, Porvoo, Finland as a background for following work on the company specifications regarding piping design and piping stress analysis.

First of all I would like to express my gratitude to my instructor Rikumatti Paldanius, for giving me the opportunity to work on this challenging task and all the support and guidance he gave me throughout the work on this thesis. Also I would like to thank Matti Tapio Hämäläinen for the valuable comments and advice during the work. Guidance of both of you greatly helped me in understanding details and background for this work.

Next, I would like to thank my supervisor professor Gary Marquis for all advice and support with the thesis.

I also wish to express the appreciation to Sergei Lemetti, Marko Väisänen, Pekka Heikkinen, and Teppo Kainulainen for helping me and providing me with all the material, advice and comments necessary for this work.

I would like to thank Halid Can Yildirim and Hardeep Rayat, your council greatly helped me during the finite element method modelling and simulation.

Also I would like to thank my parents for the support, kind words and belief in me.

Finally, I wish to thank Jaakko Sorsa, Anu Sorsa and Raine Sorsa. Your support, encouragement, patience and kind words though the years of Master's studies and especially Master's thesis gave me inspiration to move forward.

Espoo, 08.08.2013

Irina Filatova

Abbreviations

API	American petroleum institute
ASME	American society of Mechanical Engineers
CAE	Computer-Aided Engineering
EGIG	European Gas Pipeline Incident Data Group
EN	The European Committee for Standardization
PID	Piping and Instrumentation diagram
SFS	Finnish Standards Association
SI	International System of Units
SIF	Stress Intensification Factor
WRC	Welding Research Council Bulletin

Symbols

Symbol	Explanation	Unit
β	Coefficient of thermal expansion specific for operating temperature	mm/mm/°C
A_p	Cross-sectional area of the pipe	mm^2
D	Outside diameter of pipe, vessel or shell	mm
D_i	Internal pipe diameter	mm
E	Modulus of elasticity specific for operating temperature	MPa (N/mm^2)
E_a	Reference modulus of elasticity at 21°C	MPa (N/mm^2)
E_C	Modulus of elasticity at the minimum metal temperature consistent with the loading under consideration	MPa (N/mm^2)
E_h	Modulus of elasticity at the maximum metal temperature	MPa (N/mm^2)
E_w	Joint efficiency factor	1
e_n	Nominal wall thickness	mm
F_a	Longitudinal force due to sustained loads	N
f	Stress range factor	1
f_c	Basic allowable stress at	MPa (N/mm^2)

	minimum metal temperature consistent with the loading under consideration	
f_{cr}	Design stress in the creep range	MPa (N/mm^2)
f_h	Allowable stress at maximum metal temperature consistent with the loading under consideration	MPa (N/mm^2)
f_m	Maximum value of stress range factor	1
$f_{t\ ind}$	Design stress for time-independent load, calculated at room temperature	MPa (N/mm^2)
I_a	Sustained longitudinal force index	1
I_i	Sustained in-plane moment index	1
I_o	Sustained out-plane moment index	1
I_t	Sustained torsional moment index	1
i	Stress intensification factor	1
L	Length of straight line joining anchors	m
L_e	Length of the equipment subjected to thermal displacement	mm
M	Resultant moment range	N·m
M_A	Resultant moment from the sustained mechanical loads	N·m
M_c	Resultant moment from thermal expansion and alternating loads	N·m
M_C	Circumferential moment in nozzle-vessel intersection	N·m
M_i	In-plane moment due to sustained loads	N·m
M_L	Longitudinal moment in nozzle-vessel intersection	N·m

M_o	Out-of-plane moment due to sustained loads	N·m
M_T	Torsional moment nozzle-vessel intersection	N·m
M_t	Torsional moment due to sustained loads	N·m
N	Equivalent number of full displacement cycles during the expected service life of the piping system	1
N_E	Number of cycles at the maximum stress range S_E	1
N_i	Number of cycles associated with displacement stress range, S_i	1
P	Internal design gage pressure	MPa (N/mm^2)
P_a	Axial force in nozzle-vessel intersection	N
R_{all}	Allowable stress	MPa (N/mm^2)
R_{eHt}	Minimum specified value of upper yield strength at calculation temperature when this temperature is greater than the room temperature	MPa (N/mm^2)
R_m	Tensile strength	MPa (N/mm^2)
$R_{p0,2t}$	Minimum 0,2% proof strength at temperature of pipe	MPa (N/mm^2)
R_Y	Ratio of the average temperature dependent trend curve value of yield strength to the room temperature yield strength	1
S_A	Allowable displacement stress range	MPa (N/mm^2)
S_b	Stress due to sustained bending moments	MPa (N/mm^2)
S_c	Basic allowable stress at	MPa (N/mm^2)

	minimum metal temperature expected during the displacement cycle under analysis	
S_E	Displacement stress range	MPa (N/mm^2)
S_h	Basic allowable stress at maximum metal temperature expected during the displacement cycle under analysis	MPa (N/mm^2)
S_i	Stress range with N_i cycles	MPa (N/mm^2)
S_L	Stress due to sustained load	MPa (N/mm^2)
St	Stress due to sustained torsional moment	MPa (N/mm^2)
S_Y	Minimum specified yield strength at design temperature	MPa (N/mm^2)
T	Operating temperature	°C
t	Pipe wall thickness	mm
U	Anchor distance, straight line between anchors	m
V_C	Circumferential shear force in nozzle-vessel intersection	N
V_L	Longitudinal shear force in nozzle-vessel intersection	
Y	Resultant of total displacement strains to be absorbed by the piping system	mm
y	Temperature coefficient	1
Z	Sustained section modulus	mm^3
z	Joint coefficient, used for the component which include one or several butt welds; the value depends on the extent of non-destructive testing	1

Table of Contents

Analysis of nozzle flexibility in nozzle-vessel intersection

1. Introduction

1.1. Background

This work had been performed as a background for further alternation of the piping design specification in Neste Jacobs. The development of the guideline for piping stress analysis is following as well. Initially, flexibility analysis rules have been introduced in the 1955 Edition of the ASME B31 Code for Pressure Piping. The calculation routine has been rather complicated at that time. In order to perform the flexibility analysis of the piping, a quantity of manual calculations had to be done. Piping stress analysis had been accomplished in form of large tables and manual calculations. (The M.W. Kellogg Company, 1955), (Grinnell Company, Inc., 1967)

Later on, application of computers has been introduced to piping stress and flexibility analysis that simplified the stress analysis process. Nevertheless, computer analysis has been extremely expensive and time-consuming process. Therefore, only most critical lines had to be analysed with utilizing the computer power. Simpler and smaller lines had to be compared to already existing lines that had shown satisfactory performance or analysed with the manual calculations. Calculation of flexibility and stress level on that time has been exceptionally resource-consuming and expensive. With time, computer power has been growing and computer price has been decreasing. Gradually, computer modelling utilization share within the scope of the flexibility analysis has been ever rising.

Presently, piping flexibility analysis is widely applying computer means. With development of piping analysis software the stress analysis process is becoming easier. Although, considering all the complexity of software and theory behind it, model of pipeline sometimes cannot take into account all the matters and details of the real system. Thus, certain assumptions and simplifications have been agreed in the analysis.

Pipeline stress analysis composes up to 10 per cent of time spent on piping engineering project. Presently, pipeline transport is the cheapest way of hydrocarbon transporting. Compared to the other means of transport, such as rail transport, road transport and ship transport like tankers (including oil tanks, chemical tankers or gas carriers), pipelines are the rapidest one. Growing demand for fuel in emerging economies justifies the development and application of pipelines. Transportation of the hydrocarbons on long distance is typically done in large diameter pipes, working under high pressure in order to increase throughput. Pressurised pipes together with content of the pipes makes up the hazardous system. Pipelines connected to equipment, such as pressure

vessels, pumps, heat exchangers, turbines; compressors exert reactions on equipment nozzles. Reaction forces and moments, caused by thermal and pressure displacements of pipeline shall be limited in order to prevent detrimental action of the reaction loads on equipment nozzles.

In Finnish petrochemical piping design presently piping stress analysis is performed according to ASME B31.3 or EN 13480-3 standards. Both guidelines provide high level of conservatism to the calculations. In present stress analysis routine nozzle-vessel junction along with the piping supports and hangers is assumed to be rigid for simplicity of calculations. In reality, nozzles possess flexibility. According to above mentioned standards, benchmark for selecting the piping and equipment wall thickness is the maximum design load case. As a consequence, nozzle and piping wall thickness is excessively high and degrades overall flexibility of the system. Due to the high wall thickness, negative effects of the thick walled shell may come to power. Risk of brittle fracture is higher for thicker shells. The border for thin-walled vessels is no more than about one-tenth (often cited as one twentieth) of its radius. According to fracture mechanics theory, in thick-walled vessel crack nucleates and grows faster than in thin wall vessel. Thick wall vessels are susceptible to brittle fracture and it is more dangerous than ductile failure. Crack, formed due to brittle mechanism, grows rapidly and fails abruptly because the crack does not undergo the plastic stage in the fracture process. That increases the risk of the structure to fail ether under initial or working conditions.

Due to the working pressure, highly explosive character of the transported contents, and large number of welds, the aftermath and subsequent losses of pipeline system failure might be enormous. Possible sequences are casualties, environment contamination, and financial loss. To avoid the possible aftermath, fracture and burst, pipeline stress analysis shall be performed. It covers the pipeline failure due to overstress and equipment nozzle overstress. Layout and Piping group performs the piping design engineering and stress analysis. For piping stress analysis initial data is collected from civil engineering, equipment and process groups. Presently, CAEpipe 6.81 is applied for piping stress analysis. The software shows rather accurate results in terms of the resultant stresses and displacements in structure. Appropriate safety factor shall be taken during design stage and on early design calculations, because piping components cannot be assessed at the early design stage and there is no certain knowledge about how the piping will be used. (Antaki, 2003)

According to (European Gas Pipeline Incident Data Group, 2011) failure frequency per 1000 km·yr had decreased from 0,37 in 1970-2007 periods to 0,16 in 2006-2010 period on 56,5%. Presently, majority (65,1%) of the failures in pipeline systems are caused by external interference or construction defects.

Generally, piping stress analysis is done in conventional software and in case of the nozzle loads exceeding the allowable level, additional supports shall be introduced to the system or geometry of the line shall be alternated to have higher inherent flexibility. In other case, equipment manufacturer can be asked if the obtained reactions are critical or can be accepted. In critical case, FEM analysis shall be ordered. The fragment in question is modelled and simulated in FEM software. Typically, nozzle-vessel interaction is modelled and boundary conditions are imposed to simulate the real boundary conditions. The result shall show accurate nozzle loads. If the load is below the allowable value, design is accepted; otherwise the changes shall be introduced to design. Typically, the nozzle thickness would be increased or nozzle reinforcing pad shall be applied.

1.2. Focus of the thesis

Thesis is focusing on problem of piping stress analysis and nozzle flexibility factor utilizing. In most cases, during stress analysis nozzle-vessel junction is assumed to be rigid. Flexibility of the nozzle is not taken into account in stress analysis to simplify of the calculations. In real systems, nozzles normally possess significant flexibility and ignoring the flexibility in stress analysis might lead to large overvaluation of the nozzle loads. Results obtained from the calculations provide safe operating conditions for pipeline system but the calculations are conservative because of the ignored flexibility. That entails the problems of the higher wall thickness for pipeline and vessels than the optimal value. That might cause the problems of excessive weight, excessive price, susceptibility to brittle fracture, and the supporting problems. Normally, the benchmark for the piping stress analysis is ensuring the stress level is within the allowable stress range and the reactions on the connected equipment are lower than the allowable level. As the benchmark of the piping stress analysis in the thesis is the ensuring that the reactions on the connected equipment are lower than the allowable level. Typically, stress analyst checks the reaction load and compares the reactions with the allowable load level provided by equipment group. Normally, piping group is aiming for higher allowable loads with the purpose of making the pipeline design simpler and not to use additional supports to increase the flexibility and lower the reactions on the equipment. In turn, the equipment group is aiming to use lower allowable nozzle loads for equipment to keep it working safely and position to be correctly aligned.

According to (Markl, 1955), flexibility factor is the ratio of the rotation per unit length of the part in question produced by a moment, to the rotation per unit length of a straight pipe of the same nominal size and schedule or weight produced by the same moment. Thus, the flexibility factor is a dimensionless value showing how flexible certain part is comparing to the straight pipe. In this work, axial translational, circumferential and longitudinal rotational nozzle flexibilities are considered, as the corresponding nozzle

loads are critical for stress analysis, such as axial force, circumferential and longitudinal moments.

1.3. Goals of the work

This work includes two sets of goals, such as research of the nozzle flexibility factors and development of the guideline for piping stress analysis. First of all, nozzle flexibility factors shall be studied. Research of nozzle flexibility factors include the study of piping stress analysis methodology, and how the flexibility factors are utilized. Study of nozzle flexibility factors calculation methods shall be reviewed. The main goal of the work is to obtain the nozzle loads on vessel-nozzle junction in the system of piping, pressure vessels and supports from FEM model simulation. Results of the FEM simulation shall be compared to the allowable nozzle loads for each given nozzle. Based on obtained results from FEM simulation, nozzle flexibility factors shall be calculated and compared to the standard values taken from (Mershon;Mokhtarian;Ranjan;& Rodabaugh, 1987) WRC 297 bulletin guidelines.

Secondly, measures listed above shall serve as the background for development of the guideline for piping stress analysis. Precise FEM simulation results for nozzle loads shall provide the idea for refining the piping design specification. Primal goal for the company is creating the comprehensive guideline for piping stress analysis. The guideline shall be applicable for variety of software types, such as CAEpipe, F-pipe, and CAESAR II. In order to simplify the stress analysis routine, proposal for detailed input datasheet shall be introduced. In addition, systematizing the report obtained from the software and input form to decent form shall be done. Piping design rules are expected to be reviewed in order to use lower design conditions for the piping design. Currently the maximum design conditions are utilized in piping stress analysis according to (American Society of Mechanical Engineers, 2012), (EN 13480-3, 2012).

1.4. Limitations, assumptions and simplifications

In stress analysis routine, pipeline system shall be modelled in structural analysis software. The model represents the most important features of the real system such as structural geometry, material model, loads, and boundary conditions. As in any model, some of minor system features may be missing due to simplification of model and thus the computer model of the piping might be not comprehensive. Number of features is normally neglected in piping stress analysis are lines smaller than 1 inch, valves and fittings geometry, nozzle flexibility.

Simulation of the system is represented as the testing of the system's model. Therefore, once the model does not represent the complete system features, the model's simulation will not show the perfectly accurate result. However, as the model is represented by major features of the system and only insignificant features that make the simulation calculation more time-consuming are neglected, results are accurate

enough for the correct assessment. In this work main simplifications for conservative model are: nozzle is assumed rigid, line with nominal size of 1,5 inch is neglected, vessels, nozzles and vessel supports are not modelled. For FEM model simplifications are as follows: piping insulation is neglected, line with nominal size of 1,5 inch is neglected, flanges had not been modelled.

1.4.1. Material modelling

For the modelling the system in FEM software, material library had been created (see Appendix F). Material of the system is assumed to be in linear elastic region. Material is ductile and does not yield. Thus, the mechanical properties utilized in FEM simulation are elastic modulus, yield strength and the Poisson's ratio. In software the values are represented in temperature-dependent form for accuracy as the system is subjected to three load cases under different working temperature. General mechanical data for the materials applied in FEM simulation, can be found in Table 1. The data had been taken from the corresponding tables from standards, specified in brackets.

System part	Material	Yield strength, MPa (20° C)	Elastic modulus, MPa (20° C)
Piping + nozzles	A106 grade B (ASME B 31.3-2012)	172,4	203064
Lower vessel	P275NH (EN 10028-3:2009)	275	194745
Top vessel	P275NH (EN 10028-3:2009)	275	194745
Vessel supports	P265GH (EN 10028-2:2009)	265	200000

Table 1: General material mechanical properties of the system

The accuracy of the simulations depends on the accuracy of the material model of the system. SolidWorks have been used for modelling the overall system and performing the simulations. Effect on flexibility of vessels and vessel supports and nozzle had been taken into account in SolidWorks. In CAEpipe only piping and nozzles can be modelled but the material and section libraries are presented comprehensively. Material model follows classical assumptions of the strength of materials. Assumptions applied in system modelling are basic for the applied mechanics. Previous loading is not taken into account. According to strength of material theory, material of the model possesses:

1. Continuity (no discontinuities in the material, no holes or voids)

2. Homogeneity (identical properties in all point)
3. Isotropy (identical properties in all directions)
4. Deformability
5. Full elasticity
6. Material is of solid (continuous) structure
7. Small-displacement theory
8. Linear elasticity

(Lanza, 1973), (Chandramouli, 2013)

1.4.2. Loading modelling

Formal analysis shall be performed on complete systems between the anchor points where boundary conditions are known. Direction of the free movements and fixation at supports shall be simulated in the analysis. According to equipment drawing, the operating and design maximum load differ for different parts of the system (see Table 2). Pipeline-equipment connection is modelled with specified thermal displacements of the equipment. Gap between the top vessel and a base is assumed to be sliding point. In current work loading is presented by internal pressure, own weight of the piping and content, supports, thermal displacements of the connected equipment, thermal load. Three different load cases are analysed and simulated.

The wall thickness temperature is equal to fluid temperature. Vessel supports are assumed to be under ambient conditions. Flanges had not been modelled to simplify the model. However, boundary conditions created by flanges had been duplicated.

Design maximum load is the ultimate maximum temperature and pressure combination that system can attain. Operating load is the normal working temperature and pressure combination that system attains during the workload. Design minimum load is the ultimate minimum temperature and pressure combination that the system can attain.

Load case	Load condition							
	Temperature, °C				Pressure, kPa			
	Piping	Top vessel+ nozzle	Bottom vessel+ nozzle	Vessel supports	Piping	Top vessel+ nozzle	Bottom vessel+ nozzle	Vessel supports
Design maximum load case	250	285	250	21	600	500	500	Atmosphere
Operating load case	40	70	40	21	168	80	160	Atmosphere
Design minimum load case	0	0	0	-40	0	0	0	Atmosphere

Table 2: Load cases according to equipment drawings and line list

It is assumed that only sustained loads act on a system there are no occasional, dynamic or exceptional loads acting. Porvoo refinery in Finland is situated in seismically stable region, thus no seismic analysis is required. There is no cold springing in a system due to company restrictions. For present work following methods had been utilized in order to obtain the results as can be found in Table 3.

Computing method	Load cases
1. Fully rigid nozzle connection with no flexibility. Modelled in CAEpipe 6.81 using "anchor" model. Conventional method of flexibility calculations. Most conservative method.	1. Design maximum load 2. Operating load 3. Design minimum load
2. Flexible nozzle connection with axial translational, circumferential and longitudinal rotational stiffnesses modelled in CAEpipe. "Nozzle" model is used specifying vessel and nozzle characteristics. More precise and less conservative method, than fully rigid assumptions, but not taking into account supports and vessels flexibility.	1. Design maximum load 2. Operating load 3. Design minimum load
3. Comprehensive FEM of the system including the vessels and supports is built and analysed in SolidWorks 2012. Material model is comprehensive and nozzle flexibility is taken into account. Results are expected to be most accurate.	1. Design maximum load 2. Operating load 3. Design minimum load
4. Same model as 3 but with flange connections fixed.	1. Design maximum load 2. Operating load 3. Design minimum load

Table 3: Calculation methods description

The nozzle reactions and rotation values obtained for each computing method had been compared to each other and the flexibility factors had been obtained. When it is necessary to simplify the system characteristics in order to reduce the complexity of the analysis, details of such simplification shall be recorded in design calculations. When assumptions are used in calculations or model simulation; applied forces, moments and stresses, and stress intensification factors shall be evaluated (EN 13480-3, 2012). The influence and significance of all parts of the piping system to be analysed and of all restraints, such as supports or guides, including intermediate restraints serving for

reducing the moments and forces on equipment or small branch lines, shall be considered. (EN 13480-3, 2012)

Initially, Bourdon effect had not been included to piping stress analysis software, but in recent software version it has been built-in and there's possibility to include the effect to the stress analysis. Expansion of the vessel under the internal pressure load must be taken into account. If the piping is not restrained, it would not cause displacement (secondary) stresses. In case of applying the restraints or introducing more than one anchor or the support directed to the pressure expansion, causes secondary (displacement) stresses from the introduction of restraint. Stress appears in addition to longitudinal and hoop pressure stresses. The Bourdon effect tends to straighten the curved members of piping system. (SST Systems, Inc., 2012)

Assumption parameter	Value
Piping insulation	Not applied
Friction coefficient	0,4
Pipe diameter units	Inch
Unit system for the system, except pipe diameter	SI
Reference temperature	21 °C

Table 4: Assumption list

2. Literature review

2.1. State of the art

The literature research had revealed that flexibility problem of vessel-nozzle-piping interaction is recognized and had been studied. Most of the research had been published since 1955 when Markl had released the report about piping flexibility (Markl, 1955). The research had been done for both nozzle-vessel intersection and pipe branch intersection flexibility analysis. Overall scope of the research is rather wide and scattered. Flexibility had been studied for various types of nozzles, such as flush, reinforced, protruding. Also rather large deal of research had been done for nozzles connected to cylindrical and spherical vessels and vessel heads. Most of the papers study isolated nozzle-vessel intersection, not subjected to pressure. In this work nozzle-vessel connection is subjected to internal pressure that decreases the inherent flexibility of the nozzle.

The research had been done for radial flexibility of the welded-pad reinforced nozzles in ellipsoidal pressure vessel heads (Chao;Wu;& Sutton, 1985). As a result flexibility factors as functions of nozzle-vessel geometry parameters had been obtained. The work might be useful in more general case of nozzle design. However, in this work nozzles are unreinforced and connected vessels are cylindrical, thus the results of (Chao;Wu;& Sutton, 1985) work cannot be applied in this work.

More work on determination of the nozzle flexibility factor had been done for ellipsoidal pressure vessel heads subject to external moment (Chao & Yeh, 1986). The research had been based on standard equations for calculating nozzle flexibility from (Moore;Rodabaugh;Mokhtarian;& Gwaltney, 1987). The analysis had been based on a guideline for nozzles in spherical shells. Vessel heads had been studied with imposed boundary conditions on the vessel head knuckle, thus the analysis is legit. The results of the work could be applied in current work for the lower vessel-piping connection although the vessel is cylindrical, but the head is ellipsoidal. The lower vessel's nozzle flexibility can be defined with the help of the article's results. However, in research the boundary conditions applied on the head's knuckle are fixed and in current work the head knuckle is not fixed.

For calculating the nozzle flexibility factors for welded-pad reinforced nozzles on ellipsoidal pressure vessel heads (Chao;Wu;& Sutton, 1985) utilized numerical method such as equilibrium equation for elastic shell from thin shell theory. Results are represented by the graphs of flexibility factors for the most often used nozzle-pad-vessel geometries as a function of the vessel and nozzle parameters. Also, results for different types of vessel heads are represented, such as ellipsoidal, hemispherical heads. The study of the influence of reinforcing pad size and thickness had been performed. The regularity is as follows: the thicker the reinforcing pad the lower nozzle flexibility is. Also, the greater the reinforcing pad size, the lower nozzle flexibility is. In present work nozzles without reinforcement are observed but the conclusions from the research mentioned above might be applied in design of pressure vessels.

Many research papers utilize the nozzle flexibility research by (Moore;Rodabaugh;Mokhtarian;& Gwaltney, 1987) and number of other research of nozzle flexibility analysis. Work of (Moore;Rodabaugh;Mokhtarian;& Gwaltney, 1987) is a literature research developed for improvement of the nozzle flexibility analysis. The report covered the nozzles and branch connections in piping system itself and the nozzle connections of piping and cylindrical vessels. The flexibility factors had been considered. It aimed to collect and analyse the available information about flexibility analysis and nozzle flexibilities in order to improve the rules for flexibility analysis. The goal was to compare the available nozzle flexibility values and compare those to nozzle flexibility values obtained from analytical methods of calculating the nozzle flexibilities for using in piping system design analysis. Report is based on 18 reports on nozzle

flexibility, branch connection flexibility that had covered period from 1953 to 1986. The analysed data had been used in the development of ASME 1986 Code flexibility equations. For flexibility analysis, displacement and rotation data have to be obtained specifically for determining nozzle flexibility. The paper discusses the different theories of obtaining the flexibility factor for both piping branch connections and nozzle-vessel intersection. That summarized the existing data for nozzle flexibility coefficients present in 1986. Also modelling and simulation work had been conducted in code-based software (Lugs, Fast2) to prove the flexibility coefficients obtained from different theories. Based on recent software of that time, (Moore;Rodabaugh;Mokhtarian;& Gwaltney, 1987) gives rather comprehensive information on nozzle flexibility factors for reinforced and unreinforced nozzles and for different parametric models. In the work code equations for ASME Code Class I had been approved to be the most accurate. Other well-known theories such as Bijlaard's theory (Bijlaard, Stresses From Local Loadings in Cylindrical Pressure Vessels, 1954), (Osage;Straub;Buchheim;Amos;Chiasson;& Samodel, 2010), (Mershon;Mokhtarian;Ranjan;& Rodabaugh, 1987), Steeles' theory (Steele & Steele, Stress analysis of nozzles in Cylindrical Vessels with External load, 1983), (Murad & Sun, 1984) design charts of defining the flexibility factors for two intersecting cylinders or nozzle-spherical head intersection had been analysed and discussed. Bijlaard's theory proved to be applicable for defining flexibility factors for unreinforced nozzle but gave inadequate results for reinforced nozzles. However, Bijlaard theory is developed for rigid cylindrical block on vessel, representing nozzle and the theory does not include the opening in a shell. Nevertheless, the Bijlaard theory gives reasonably accurate results. For each type of branch connection and based on parametric data the comparison had been made based for different theories and for Lugs, Fast2 software. The research of the interest had been obtained for the models under internal pressure. Benchmark had been experimental data obtained from (Cranch, 1960). The report also provides the research of the nozzle flexibility of the junction subjected to pressure. Research results showed that the nozzles subjected to pressure possess lower flexibility.

Similar with this Master's thesis work had been done by (A. Hardik & Trivedi, 2011). Stress analysis of reaction nozzle to spherical head junction had been performed. Radial and tangential membrane and bending stresses had been calculated for eight points at nozzle-vessel junction based on WRC 107 Bulletin. The obtained results had been validated in code-based software and both calculation ways showed that the design would fail because the resultant stresses were exceeding the allowable stress level. Then the nozzle-vessel junction part had been modelled and simulated in FEM software. The results had been compared. Results obtained from FEM simulation fell under allowable load level. Due to calculation routine in WRC 107 that does not take pressure load into account, and calculated stresses due to pressure thrust of membrane

theory is added algebraically to the calculated stress. FEM results obtained from ANSYS are more accurate than WRC 107 and code-based software (PV-Code Calc). The results are calculated for the whole junction in FEM software and not only for eight points like in WRC 107. The (A. Hardik & Trivedi, 2011) work is equivalent to present Master's thesis in methodology and means of obtaining the results. The difference is in applied software and in present work WRC 297 had been utilized. However, the (A. Hardik & Trivedi, 2011) work can be useful in determining the methodology and scope of work and routine of nozzle load calculation. The work is utilizing similar principle as the current work. Comparison has been conducted between the nozzle loads on junction, calculated according to WRC bulletin rules, piping code calculations, and FEM analysis. The work is represented for spherical vessels and heads, whilst current work is considering the cylindrical vessels. The scope of work is limited due to the scale. Thus, only for one case the modelling had been conducted and compared with other methods of determining the stress.

Similar with this work methodology had been applied in (Schwarz, 2004) work. In the work stiffness coefficients for cylindrical and spherical vessel intersections with piping have been acquired from WRC 297 and BS PD 5500 Appendix G. Also, the stiffness coefficients have been obtained from FEM simulations of the vessel-piping interface. The stiffness coefficients obtained from WRC, BS and FEM simulations have been compared. In general, obtained results showed good correlation for the thick walled nozzles (wall thickness ratio T/t = 0,5) and under certain parameters good agreement in other cases. The results had been computed for parametric model based on geometric characteristics of nozzle and vessel. Particular interest for current work is in the axial, circumferential and longitudinal moment flexibility factors for cylindrical vessel. The results have been yielded from more than 1000 FEM models built and simulated. Simulations have been conducted with the purpose of expanding the result range for wider geometry application than existing diagrams in WRC 297.

Problem of conservative calculations assuming the nozzle rigid had been considered in other industries as well. Work of (Weiss & Joost, 1997) sets the problem of the excessive nozzle rigidity and compliance-constants for piping design have been developed. Compliance-constants for three types of nozzles had been computed: flush nozzle, reinforcing pad, protruded nozzle. Pad reinforced nozzle possesses the highest inherent rigidity, protruded nozzle has lower rigidity and the lowest rigidity is characteristic for flush nozzle. The work yielded the reasonably accurate results based on FEM simulation of quarter of the nozzle-vessel intersection. The results of the work are possible to utilize in present Master's thesis for flush nozzle and cylindrical vessel. The compliance-constants are represented as parametric equations and thus may be used for various geometries. The further work can be done is to expand the range of design cases. Presently, only t/T=0.5 and t/T=2 are presented.

The research had shown that rather wide work had been done in the nozzle flexibility research. Mostly methodologies of work are based on determining the flexibility factors based on equations from the rulebooks and standard codes, and then comparison of the results from code-based software and FEM software that is considered to be the benchmark in most of the cases. In (Moore;Rodabaugh;Mokhtarian;& Gwaltney, 1987) the benchmark data is the set of experimental test results of nozzle flexibility conducted by (Cranch, 1960). The results normally agree rather well, but mostly show the conservatism of code-based software and rulebooks based calculation results. Present tables and results are limited by certain parameter set that does not cover the whole possible range of the nozzle-vessel parameters. Also, all above mentioned works consider in FEM simulation only quarter or half of the nozzle-vessel interaction with imposed boundary conditions. In real life, normally there are supports on the vessel and above the vessel there is piping with supports or hangers. Also, the internal pressure decreases the nozzle flexibility and it had been mentioned only in (Moore;Rodabaugh;Mokhtarian;& Gwaltney, 1987) work, while the rest works make research based on the nozzle-vessel junction not subjected to pressure. This work takes into account the comprehensive piping model including the vessel supports, piping and vessels in order to find the correct nozzle loads. Also, full-scale modelling had been conducted for all possible design cases, including the pressure, temperature and deadweight. Therefore, the rather accurate results can be expected.

2.2. WRC Bulletin 297 and 107

WRC Bulletins are widely used in pressure vessel design. WRC 107 is a guideline containing diagrams and equations intended for calculating local stresses in spherical and cylindrical shells due to external loadings and do not contain the equations for local stresses in nozzles. WRC 297 contains the guidelines for calculating local stresses in cylindrical shells and nozzles due to external loadings and broadens the range of geometrical factors covered in Bulletin 107 and includes stresses in the nozzle at the nozzle-vessel intersection. 107 Bulletin gives instructions for calculating the local stress in nozzle-vessel intersection vicinity, and WRC 297 in addition to the local stresses gives the instructions for nozzle flexibility calculation. WRC 107 considers the un-penetrated shells and WRC 297 studies the shells with circular openings. WRC 107 distinguishes the different cases of hollow and solid nozzles for spherical shells but does not distinguish that for cylindrical shells. Also WRC 107 is based on assumption that the nozzle is a rigid solid rectangular attachment to a vessel. WRC 297 in turn is intended only for cylindrical shell and cylindrical nozzle intersection. The calculation is based on a prof. Bijlaard's thin shell theory. Thin shells are those, in which deformations are not large compared to the thickness. Bijlaard theory considers nozzles as a rectangular solid insert to the shell. To adjust the theory for the opening in shell (Mershon;Mokhtarian;Ranjan;& Rodabaugh, 1987) para.3 equations are applied. For calculating the local stresses number of diagrams is present in WRC 297 report. For

nozzle flexibility calculations diagrams with nozzle stiffness coefficients based on geometrical parameters of nozzle and vessel are presented. Diagrams in Bulletin present axial translational, circumferential and longitudinal rotational stiffnesses that represent the most critical nozzle parameters and thus is valid for utilizing in this work. As this work is focusing on nozzle flexibility analysis, figures 59 and 60 from WRC 297 are utilized in the work for nozzle stiffness calculation. The data for the figures 3-58; 59 and 60 is taken from Shelltech report 80-2 (Steele & Steele, Stress analysis of nozzles in Cylindrical Vessels with External load, 1983), (Steele;Steele;& Khathlan, 1986). in the Bulletin guidance for calculating stresses caused by torsion and shear forces but they can be conservatively assumed to be constant maximum calculated value.

WRC 297 is based on Steele's theory that is applicable to only those nozzles which are normal to a vessel surface and for the systems where both vessel and nozzle fall under thin shell theory. According to WRC 297 and (Steele & Steele, 1983), the thin shell theory is valid for the systems with the following parameters: d/t ≥20, D/T≥20 and d/T≥5 and D/T≤2500. The Bulletin provides the graphs for d/t≤100 because it had been assumed that this will cover most of the nozzle types in vessels or piping. Steele's theory is applicable to isolated nozzles that are sufficiently remote from the stress discontinuities such as the openings in the vessel or nozzle. Distance of $2\sqrt{DT}$ on the vessel or $2\sqrt{dt}$ on the nozzle provides sufficient distance to deliver reasonable design guidance. Theory is not applicable for nozzles protruding inside the vessels. The nozzle must be welded to the vessel by a full penetration weld. For this work WRC 297 had been used because both vessels are cylindrical and data provided in WRC 297 is more comprehensive than in WRC 107.

Curves from figures 59-60 of (Mershon;Mokhtarian;Ranjan;& Rodabaugh, 1987) had been used for the determining the nozzle flexibility. However, the curves on the mentioned figures are provided for only limited range of parameters with nonlinear dependency and the result is dependent on several parameters that make complication for interpolation. Data on the figures is fairly limited. The values in the curves are valid for the simply supported shells with ends round but free to rotate. Also, the WRC warns that the interpolation of the curves or using the other types of boundary conditions may lead to significant inaccuracies. Disadvantage of the usage of WRC Bulletins is that the guidelines are given for vessel-nozzle with no pressure. As a matter of fact, most of the vessels in petrochemical industry work under the pressure, different from atmospheric. According to (Moore;Rodabaugh;Mokhtarian;& Gwaltney, 1987), internal pressure decreases the flexibility of the nozzle. Thus, the results obtained from WRC calculation might be assumed underestimated.

2.3. EN 13480: Metallic Industrial Piping – Part 3: Design and calculation

In piping flexibility analysis EN 13480-3 is one of the several national standards giving the guidelines for performing the analysis. EN 13480 Metallic industrial piping – part 3: Design and calculation is a part of seven parts of the EN 13480 Standard and it has the status of national standard. The standard gives the general guidance for design and calculation of metallic industrial piping and supports. Basic parts of piping design and calculation routine are given as well as the general piping flexibility analysis instruction. For this work the flexibility analysis procedure from the standard is utilized. Also, piping stress analysis software calculations are based on the flexibility analysis procedure from EN 13480-3. Besides that, wall thickness calculations can be found in standard.

According to EN 13480-3, piping shall possess appropriate flexibility in order to not create excess reactions on equipment nozzles and prevent any excess sag. Sufficient flexibility can be achieved by applying certain support types, hangers, spring hangers, guides and expansion loops. Expansion joints as well help to increase the piping flexibility. With the aim of acknowledging the pipeline system to be adequately flexible, using the equations the Standard requires longitudinal moment stress range to be restricted to be less than certain allowable value. Equations for the stress range are given in the standard and the allowable value is determined on the basis of national or corporative standard. In piping design EN 13480-3 is used for wall thickness calculations and is based on maximum design pressure and temperature combination.

2.4. ASME B31.3: Process Piping

Second most widely applied standard is the American Standard of Mechanical Engineers is applied for petrochemical, oil, gas and chemical process piping. It is most widely used for flexibility analysis as a guideline. The basic rules for piping design are given as well as in EN standard but with more attention on process piping under high pressure. Unlike the EN standard, ASME provides the tables with mechanical properties of most commonly used in petroleum service piping steel types and with allowable stresses presented in a form of temperature-dependent data. Also the design and calculation rules are presented in the standard that is favourable to be followed in the petroleum service. Basic guideline for piping flexibility analysis is presented and can be used in this work. Also, guidelines for wall thickness calculation can be used. Basics of the flexibility analysis and piping design and calculation, such as stress range, stress limits, piping wall thickness are presented in both EN and ASME standards and gives comparative results. However, in process piping engineering ASME B31.3 is primarily followed in flexibility analysis and EN 13480-3 is rarer. Also, presented guidelines for flexibility analysis are the base for piping stress analysis software. However, in ASME B31.3 standard is presented the equation for checking whether the system falls within the limitations of the equation 1:

$$\frac{DY}{(L_1-U)^2} \leq 208{,}3 \qquad (1)$$

Where

D = outside diameter of pipe, mm;

Y= resultant of total displacement strains to be absorbed by the piping system, mm;

L_1 = developed length of piping between anchors, m;

U= anchor distance, straight line between anchors, m;

If the system falls within the limitation of the equation 1 and has no more than two restraints, the formal flexibility analysis is not required. Nevertheless, the equation 1 is empirical and does not provide the accurate enough results and cannot be used for any complex piping system. Nonetheless, the equation 1 is mentioned in many piping design textbooks and is presently referred to (Holmes, E.; Rodger, C. D.; Halligan, B. D.; Westerman, V.; Lander, D. W.; Madden, J.; Masters, E. H.;, 1973), (The M.W. Kellogg Company, 1955).

2.5. Comparison of pipe wall thickness calculated according to EN 13480-3 and for ASME B 31.3

Let us compare the wall thickness values obtained for the same initial conditions. Wall thickness will be calculated without allowances and tolerances for straight pipe under internal pressure.

Material is A106 Grade B;

D = 355,6 mm;

Design temperature = 250 °C;

Design pressure = 600 kPa;

Yield Strength = 241 MPa;

Yield Strength at 250°C;

Tensile Strength = 414 MPa

2.5.1. Wall thickness for basic pressure piping design (straight pipe) according to ASME B31.3

Equation for the wall thickness without a tolerance and allowance is:

$$t = \frac{PD}{2(SEw+Py)} \qquad (2)$$

t = minimum required wall thickness, excluding manufacturing tolerance and allowances for corrosion (mm);

S = allowable stress level for the corresponding material consistent with operating temperature;

P = internal design gage pressure;

D = outside pipe diameter;

E_w = joint efficiency factor, 0,6≤E≤1,0; (ASME B31.3: Process Piping, 2012, s. 333)

y = temperature coefficient, 0≤y≤0,7; (ASME B31.3: Process Piping, 2012, s. 20)

S = 132 MPa;

E_w = 1;

y = 0,4;

$$t = \frac{0{,}6\ MPa \cdot 355{,}6\ mm}{2(132\ MPa \cdot 1 + 0{,}6 MPa \cdot 0{,}4)} = 0{,}81\ mm$$

After wall thickness had been determined, the allowance must be defined. The allowance must be defined for the mill tolerance and for the corrosion allowance. The thickness is taken from the piping code and then all allowances must be considered. (American Society of Mechanical Engineers, 2012, s. 20)

2.5.2. Wall thickness calculation for basic pressure piping design (straight pipe) according to EN 13480-3

According to (EN 13480-3, 2012, s. 19), minimum required wall thickness for a straight pipe without allowances and tolerances shall be calculated as stated by following equation 3:

As $D/D_i \leq 1{,}7$:

$$t = \frac{PD_0}{2R_{all}z+P} \qquad (3)$$

Or

$$t = \frac{PD_i}{2R_{all}z-P} \qquad (4)$$

D_i – internal pipe diameter;

$$R_{all} = min\ \{\frac{R_{eHt}}{1,5}\ or\ \frac{R_{p0,2t}}{1,5}\ ;\ \frac{R_m}{2,4}\} \qquad (5)$$

R_{eHt} = minimum specified value of upper yield strength at calculation temperature when this temperature is greater than the room temperature, MPa;

$R_{p0,2t}$ = minimum 0,2% proof strength at temperature of pipe, MPa;

R_m =Tensile strength, MPa;

z = joint coefficient, used for the component which include one or several butt welds; the value depends on the extent of non-destructive testing; 0,7≤z≤1

$$\frac{R_{eHt}}{1,5} = \frac{164\ MPa}{1,5} = 109,3\ MPa;$$

$$\frac{R_m}{2,4} = \frac{414\ MPa}{2,4} = 172,5;$$

R_{all} = 109,3 MPa;

z = 1;

$$t = \frac{p_c D_0}{2R_{all}\ z+p_c} = \frac{0,6\ MPa \cdot 355,6\ mm}{2 \cdot 109,3\ MPa \cdot 1+0,6\ MPa} = \frac{213,36\ MPa}{219,8} = 0,97\ mm \qquad (6)$$

Thus, EN 13480-3 standard gives more conservative result for pipe wall thickness and basically higher values for the wall thickness. Normally, EN 13480 is a general service standard for general piping, thus it gives conservative results. ASME B31.3 is more specific Code for Process piping, thus it gives more precise results.

3. Industrial best practice

Presently, number of different piping stress analysis software is utilized in industry. It significantly reduces the time spent on piping design, cost of maintenance and allows checking different alternatives of design arrangements fast. Most widespread software types for petroleum service are as follows: CAESAR II, CAEpipe, F-pipe, Triflex, ROHR2, AutoPIPE. Generally, all software types are Code-based and give the results as the comparison between the allowable and sustained stress. Most of the software types are similar in format of input and output. However, the scope of the analysis can vary for different software types, for example, stability or dynamic analysis.

Different software types vary by the scope of the analysis. For example, CAESAR II does include the stability analysis but CAEpipe does not. CAEpipe is also considered to

be the best software for fast processing of large amount of data. CAESAR II is acknowledged for its accurate results and user-friendly interface. (Intergraph CADWorx and Analysis Solutions, 2007), (Animated Tutorials, 2013). Moreover, both software types can provide the dynamic analysis that is missing in other types of software.

According to (SST Systems, Inc., 2012), CAEpipe analysis can be submitted for number of Codes, also work well with the nozzle flexibilities. Significant advantage is the possibility of the import of the models from design software or other stress analysis software. However, modelling of the vessels and vessel supports is not provided, that make results conservative and overestimates, especially on nozzles.

The disadvantage of the CAEpipe software is the impossibility of proper modelling of the nozzle-vessel connection of the piping. However, there is a function "nozzle" that takes into account axial, in-plane and out-of-plane nozzle flexibilities. Normally, the nozzle connections are assumed to be rigid and depicted as "anchors" in software. Next disadvantage is impossibility of modelling the vessel and vessel supports. Those are assumed rigid and this brings more conservatism to the calculations. Second major disadvantage is not comprehensive material library. Nevertheless, it can be edited manually by adding the missing properties to library or creating the custom library. Thus, the accuracy of the calculated nozzle loads and support loads is not sufficient. However, obtained results can be utilized in piping design as they are conservative and give reasonable safety margin. On the other hand, the problem of the software is rather high conservatism of obtained results.

Autopipe software does provide the code-based analysis but disadvantage of the software is missing certain features such as dynamic analysis. The advantage is the possibility of converting the model directly from PDS (Plant Design Software) to Autopipe and that batch file will include the vessels connected to pipelines. Also, supports modelling are more advanced than in CAEpipe.

The basics of the piping stress analysis is an expansion of piping under the thermal and pressure load, dead weight of piping, fluid and internals, influence of the supports and external and exceptional loads on piping and influence of the above mentioned factors on the piping reactions and moments on the equipment nozzles. The piping stress analysis software normally gives reliable results based for static and dynamic analysis. The result is presented in set of displacements, forces, moments, stresses in the piping system. Generally, stress compliance, reaction forces and moments exerting by piping on the equipment are of the interest for stress analyst. Advantages of utilizing piping stress analysis software is the speed of calculations, in-built libraries of materials and valves, code, parts and pipe sections library; accuracy of obtained results and the possibility of rapid checking of different scenarios.

Disadvantages are impossibility of modelling the vessels and vessel supports and conservatism of calculations. Nozzle and flange connections are assumed to be rigid, that make the overvaluation of the acting nozzle loads on several orders. The conservatism decreases the accuracy of the calculations that leads to excessively high reactions or moments on the equipment nozzle. Commonly, the reactions and moments on the equipment nozzles are critical part of the calculations.

Equipment manufacturers or equipment engineering group in company provide the prescribed allowable level of forces and moments that equipment nozzles can withstand. Equipment manufacturers aim to assign low allowable nozzle loads and moments and simultaneously piping engineers request higher allowable nozzle loads on equipment because that would allow piping engineer to be more flexible in solutions and would impose less constraints on the system. Normally, piping system is designed or renovated to be placed to limited space available. Due to flexibility requirements, expansion loops or other design solutions can be applied to improve the flexibility and in case of limited space it is not always possible. Thus, low allowable nozzle loads can create a problem with piping flexibility especially if the piping is to be installed into limited space.

Problem of modern state of piping stress analysis is conservatism of the calculation way. For petroleum pipeline engineering wall thickness calculation is based on design load, thus the wall thickness might be excessive as a consequence. That problem is topical for both piping and pressure equipment. Also, the allowable nozzle load is normally rather conservative value and creates difficulties with piping design to provide nozzle reactions to be lower than allowable. Design temperature is an ultimate maximum or minimum of possible operating process temperature. Normally, pipelines operate under the operating load. Design temperature can be achieved by the piping system only in extreme cases such as safety valve failure or system fault.

According to the report of European Gas Pipeline Incident Data Group [10], failure frequency per 1000 kilometer·year had decreased from 0,37 per 1000 km·yr in 1970 to 0,16 per 1000 km·yr in 2010. Reasons that have been considered in report are distinguished by external interference that makes up major part of all incidents considered, corrosion, construction defect/material failure, hot tap made by error, ground movement and other reasons that include design error, lightning, maintenance. Although, design error, corrosion or construction defect do not make up significant of the incident cause (39,4%) and major part is represented by external interference, such as digging or ground works, the incident frequency rate is steadily decreasing. However, it is arguable how the incident frequency connected with stress analysis implementation, as the most incidents are external interference that is pure mechanical impact that is not possible to predict or prevent. Therefore, stress analysis does not cover this kind of

failures. Nonetheless, piping design can be classified as design error. Implementation of piping stress analysis has helped to improve the pipeline performance.

Company experience in applying piping stress analysis software shows positive effect on work efficiency and safety of designed structures. Furthermore, utilizing the piping stress analysis software helps the company's client save resources by preventing the accidents. Besides the financial damage, accidents might cause environment contamination or casualties.

In company CAEpipe, CAESAR II and F-pipe stress analysis software have been used for years and that succeeded the conventional piping stress analysis method, such as utilizing tables and manual calculations, that would be extremely time-consuming and would be suitable only for the most critical or simple lines. (King, 1967), (Grinnell Company, Inc., 1967)

Presently, there are no real alternatives in piping engineering for utilizing of the piping stress analysis software except above mentioned or rules of sound engineering practice or comparison of the new or renovated line with existing line that had shown satisfactory performance. Therefore, the piping stress analysis utilizing the piping stress analysis is an essential part of piping design process. During computerized piping stress analysis, stress level shall be checked to be below the allowable level and the loads on the equipment nozzles shall be checked to be lower the allowable level provided by equipment manufacturer or equipment engineering group as the most critical parameters of the system.

In pipeline system improper supporting of the pipe can cause pipe sag. In sagged sites conveyed fluid or condensate can be collected and cause the corrosion and/or stress concentration. As a more critical consequence, improperly supported and thus sagged areas of the piping impose increased reaction on equipment nozzle that can be detrimental. Utilizing the software for checking stress level and/or nozzle loads can prevent the sag of the pipe by modelling the supports and with the help of software it is possible to find the optimal support type and location.

Pipelines normally work under internal pressure and thermal load. Pipeline expansion caused by operating pressure and temperature influences on the system overall flexibility. Expansion and contraction of the piping influence on the nozzles of the equipment, thus proper application of supports, anchors and hangers shall be performed. Temperature gradient through the pipe wall is unwanted effect that worsens with increasing of the wall thickness. Excessive conservatism of the calculations on the design stage can introduce the unnecessary high wall thickness.

Another point is that normally there are different combinations of loads, and for each one there is a (temperature, pressure) set, such as design maximum/minimum,

operating, full load, partial load, shut-downshut-down, start-up, switching and shut-down operations. Mechanical properties of piping material are temperature-dependent. Risk is in the loss of strength on high operating temperature and loss of fracture toughness under low operating temperature. For each material nil-ductility temperature shall be taken into account, particularly, for low temperature range. Sets to be calculated shall correspond to the most severe conditions of coincident pressure and temperature which may prevail over a long time. (EN 13480-3, 2012)

4. Methodology

This section explains the means of achieving goals of this work. Test environment, models and methods can be found in this chapter. The research can be divided onto two stages. First is the scientific article research and studying the state of art and background available. Next, building a computer model software environment and model simulation has been done in order to acquire the nozzle reaction. Obtained results had been analysed based on guidelines given in WRC 297, compared and the conclusions had been made.

First part was building the model in CAEpipe 6.81 software that is code-based software used for checking the stress level and nozzle reactions in pipelines. Two different models had been built: first is the model with maximum conservative assumption, representing the basic state of the modern piping stress analysis method, that is nozzles and flanges are assumed to be fixed points. Second model had been built in CAEpipe is the same piping system with the modelled flexible nozzles. However, both models do not represent the connected vessels and vessel supports and that brings the conservatism to the results. Obtained results for the simulation are nozzle loads and displacements. The results are taken as the loads on the flange for the rigid model and on the nozzle-vessel intersection for flexible connection. The software computes the axial translational, circumferential and longitudinal rotational flexibilities for the nozzles based on geometrical data of the nozzle and the vessel. The calculations are based on (Mershon;Mokhtarian;Ranjan;& Rodabaugh, 1987, ss. 69-71) guidelines. The models built in CAEpipe 6.81 can be found in Appendix A and B.

Second part was building the model of the piping system in SolidWorks 2012 environment. The system had been represented with the maximum detailed accuracy, including piping, reducers, nozzles, vessels and vessel supports. The vessels, piping and nozzles had been modelled as shell elements. Supports on the top and lower vessel had been modelled as solid elements. Shell assumption had been made as the shell elements of the system fall under the thin shell theory and can be specified as thin shell structures. The material model had been reproduced in details in a form of temperature-dependent data (see Appendix G). The model had been simulated in FEM module of the software with fine mesh in the nozzle-vessel juncture vicinity and with

coarser mesh on large parts. The design and operating load cases had been simulated and boundary conditions had been imposed in accordance with the real system. The outcome is the reaction and moments at the nozzle connections, displacements. The outcome also had shown the behaviour of the system under three different load cases. There are three flexibilities of interest: axial translational, circumferential and longitudinal rotational. The model if the system can be found in Appendix C. Forces and moments on the nozzle can be found from the Figure 1.

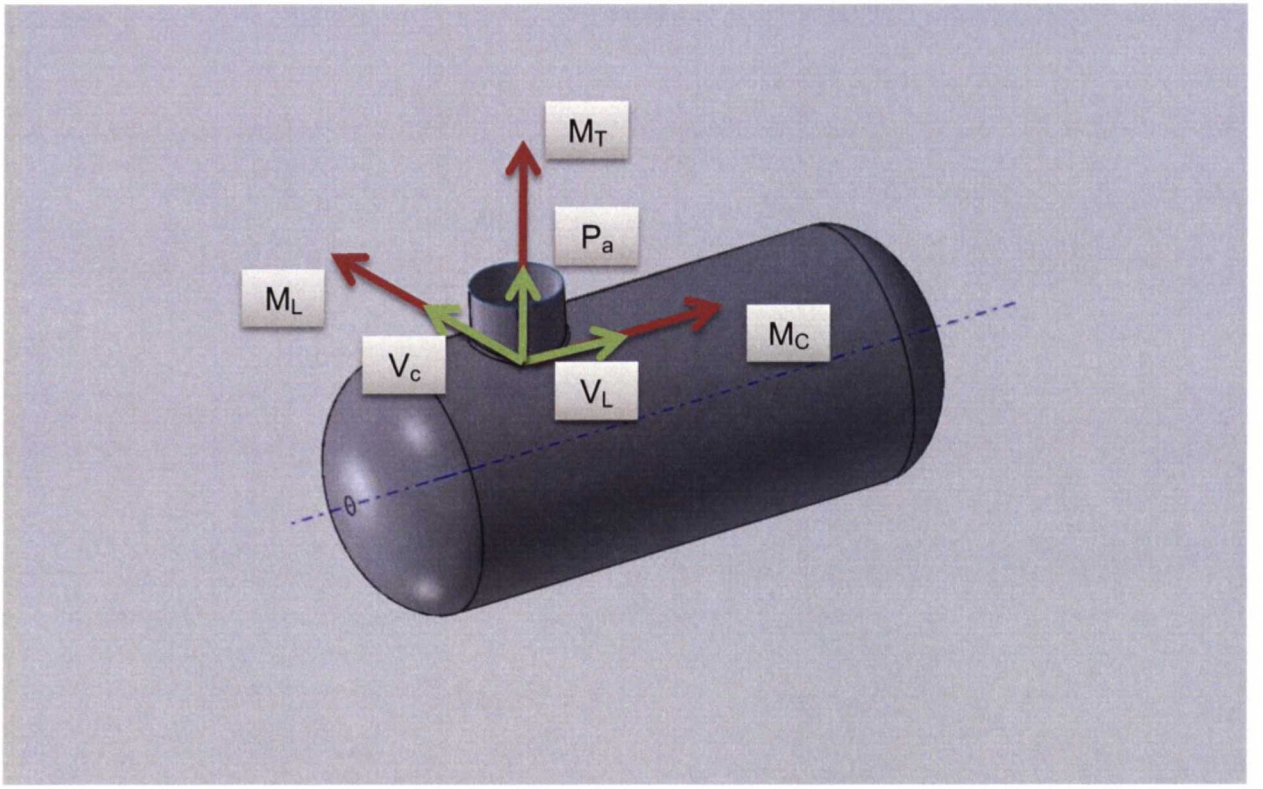

Figure 1: Forces and moments on the cylindrical nozzle - cylindrical vessel intersection

Three load cases have been analysed within the scope of this work: design maximum, operating and design minimum load, according to specified conditions for each part of the system. Intermediate load cases such as partial load, shut-downshut-down, start-up, switching and shut-down operations had not been included in the scope due to the small frequency of these events. The load cases include operating temperature, pressure and boundary conditions. In SolidWorks comprehensive FEM model had been modelled and simulated. More detailed information about the model can be found in "Model description" chapter. Static study had been performed on the model. The internal pressure had been applied on the shells as equally distributed. The temperature had been applies on the shells as equally distributed as well. The support conditions had been modelled in accordance with the specified data. As the structural model built in SolidWorks environment is rather comprehensive, only with minor parts neglected,

the system is assumed to be valid. Material model and the loading modelling had been approached to real life conditions of the system, thus the results are expected to be accurate.

General study of piping system flexibility had been performed. Influence of the flange fixture had been studied. Two cases had been considered: flange connections fixed and flange connections not fixed. The main outcome of this work is the research of the nozzle flexibility and the factors influencing the nozzle stiffness shown on the example of the real-life piping system.

4.1. Requirement for flexibility analysis

Nozzle flexibility analysis is an essential part of the piping flexibility analysis. Besides the stress level examination, nozzle loads are normally checked to be lower than corresponding allowable nozzle loads on the connected equipment. In scope of this work the nozzle flexibility analysis is taken into account. However, below the background for method of the piping stress analysis software CAEpipe 6.81 is given.

As a basic requirement of the piping design code (ASME B31.3: Process Piping, 2012), piping system shall possess sufficient flexibility to prevent thermal expansion or contraction or movements of piping supports and terminals from causing

1. Failure of piping or supports from overstress or fatigue;
2. Leakage at joints;
3. Detrimental stresses or distortion in piping and valves or in connected equipment (pumps and turbines, for example), resulting from excessive thrusts and moments in the piping

(ASME B31.3: Process Piping, 2012)

4.1.1. Formal flexibility analysis not required

No formal analysis of adequate flexibility is required for a piping system which

1. Duplicates, or replaces without significant change, a system operating with a successful service record;
2. Can readily be estimated adequate by comparison with previously analysed systems;
3. Is of uniform size, has no more than two points of fixation, no intermediate restraints, designed for a service of not more than 7000 full cycles and falls within the limitations of equation 1

According to company rules, all pipe of nominal size larger than 6 inches and working under temperature higher than 150°C shall be subjected to stress analysis. However, the equation 1 is a controversial among the piping stress analyst as it is suitable only for

simple systems with no more than two anchoring restraints, no intermediate restraints, thus only limited number of the lines can actually fall within this requirement limitation. In addition, the code itself has the note saying that there is no guarantee that equation 1 will yield sufficiently conservative and accurate results.

Piping can be checked with equation 1 and results are as following:

$$\frac{D \cdot Y}{(L_1 - U)^2} \leq 208{,}3;$$

$$0{,}00017 \leq 208{,}3;$$

As we can see, the condition of the equation 1 is fulfilled and thus according to (EN 13480-3, 2012), formal flexibility analysis is not required. However, according to company rules, piping system nominal size is larger than 6 inches outside diameter and design temperature is higher than 150°C. Therefore, the system shall be subjected to piping stress analysis.

4.1.2. Formal flexibility analysis required

Piping systems that don't meet the criteria mentioned above must undergo an analysis that could be simplified or approximate or comprehensive. A simplified or approximate method may be applied only if used within the range of configurations for which its adequacy has been demonstrated. Acceptable comprehensive methods of analysis include analytical and chart methods which provide an evaluation of the forces, moments, and stresses caused by displacement strains. Comprehensive analysis shall take into account stress intensification factors for any component other than straight pipe. Credit may be taken for the extra flexibility of such a component. (EN 13480-3, 2012)

4.2. Flexibility analysis methodology

In this section methodology for stress analysis method used in CAEpipe software will be explained. In CAEpipe stress analysis routine can be based on selected code. Most of the codes follow similar principles but safety factors for different kinds of stress range such as time-dependent stresses or stresses caused single non-repeated movement or stress caused by alternating loads can differ for various codes. According to (ASME B31.3: Process Piping, 2012), the stress analysis routine performed in CAEpipe software, following certain principles. Piping system shall meet the following specific requirements

1. The computed stress range at any point due to displacement in the system shall not exceed the allowable stress range;
2. Reaction forces shall not be detrimental to supports or connected equipment;

3. Computed movement of the piping shall be within any prescribed limits, and properly accounted for in the flexibility calculations

If it is determined that a piping system does not have adequate inherent flexibility, means for increasing flexibility shall be provided. (ASME B31.3: Process Piping, 2012)

4.2.1. Limits of calculated stresses due to displacement

4.2.1.1. Allowable displacement stress according to B31.3

Allowable displacement stress range, S_A shall be calculated in accordance with equation 7. The computed displacement stress range, S_E, in a piping system shall not exceed the allowable displacement stress range, S_A.

$$S_A = f(1,25S_C+0,25S_h) \quad (7)$$

When S_h is greater than S_L, the difference between them may be added to the term $0.25S_h$ in equation 7. In that case, the allowable stress range is calculated by equation 8.

$$S_A = f\,[1,25(S_C+S_h) - S_L] \quad (8)$$

Where

f = stress range factor, calculated by equation 9;

$$f = 6.0(N)^{-0.2} \leq f_m=1,2; \quad (9)$$

$0,15 \leq f \leq 1,2$;

f_m = maximum value of stress range factor; 1,2 for ferrous materials with specified minimum tensile strengths ≤ 517 MPa and at metal temperatures ≤ 371 ° C;

N = equivalent number of full displacement cycles during the expected service life of the piping system;

S_c = basic allowable stress at minimum metal temperature expected during the displacement cycle under analysis = 138 MPa maximum;

S_h = basic allowable stress at maximum metal temperature expected during the displacement cycle under analysis = 138 MPa maximum;

When the computed stress range varies, whether from thermal expansion or other conditions, S_E is defined as the greatest computed displacement stress range. The value of N in such cases can be calculated by equation 10:

$$N = N_E + \sum(r_i^5 N_i) \quad for\ i = 1,2,\ldots n \quad (10)$$

Where

N_E = number of cycles of maximum computed displacement stress range, S_E;

N_i = number of cycles associated with displacement stress range, S_i;

$r_i = S_i/S_E$;

S_i = any computed displacement stress range smaller than S_E

(ASME B31.3: Process Piping, 2012, ss. 15-18)

4.2.1.2. Allowable stresses according to EN 13480-3

The allowable stress range f_a shall be defined by

$$f_a = f(1{,}25f_c + 0{,}25f_h)\frac{E_h}{E_c} \qquad (11)$$

Where

E_C = the value of the modulus of elasticity at the minimum metal temperature consistent with the loading under consideration;

E_h = the value of the modulus of elasticity at the maximum metal temperature;

f_c = the basic allowable stress at minimum metal temperature consistent with the loading under consideration;

$$f_c = min\ \{ R_m/3\ ;\ f_{t\,ind} \} \qquad (12)$$

$f_{t\,ind}$ = design stress for time-independent load, calculated at room temperature;

f_h = allowable stress at maximum metal temperature consistent with the loading under consideration;

$$f_h = min\ (f_c;\ f;\ f_{cr}) \qquad (13)$$

Where

f_{cr} = design stress in the creep range at temperature t_c (not considered within the scope of this project);

f = stress range reduction factor, may be taken from the 12.1.3-1 table from (EN 13480-3, 2012) or calculated in accordance with equation 14:

$$f = 6{,}0N^{-0{,}2} \leq 1{,}0; \qquad (14)$$

$0{,}5 \leq f \leq 1{,}0;$

Where

N = number of equivalent full amplitude cycles during the expected service lifetime of the piping system;

If the range of temperature change varies, equivalent full temperature cycles shall be as follows:

$$N = N_E + \sum_i (r_i^5 N_i) \quad (15)$$

Where

N = equivalent number of cycles;

N_E = number of cycles at full temperature change Δt_E for which stress from thermal expansion σ_3 has been calculated;

N_i = number of cycles at lesser temperature changes Δt_i;

r_i = ratio of lesser temperature changes to that for any which the stress σ_3 has been calculated $\Delta t_i/\Delta t_E$.

(EN 13480-3, 2012, ss. 41, 255-257)

As can be seen, both standards give similar guidelines for calculating allowable stress ranges, differing only for calculating of stress reduction factor. In ASME maximum value of stress reduction factor is 1.2, allowing taking into account favouring condition not subjected to hot temperature service. For EN 13480-3 maximum stress reduction factor is 1,0, that make the equation to be more conservative due to wider application of the EN standard.

4.2.2. Stress due to sustained loads

4.2.2.1. Stress due to sustained loads according to ASME B31.3

The equation for the stress due to sustained loads, such as pressure and weight, S_L, is provided in equation 16.

The equation for the stress due to sustained bending moments, S_b, is provided in equation 17.

$$S_L = \sqrt{(|S_a| + S_b)^2 + (2S_t)^2} \quad (16)$$

$$S_b = \frac{\sqrt{(I_i M_i)^2 + (I_0 M_0)^2}}{Z} \quad (17)$$

Where

I_i = sustained in-plane moment index. In the absence of more applicable data, I_i is taken as the greater of $0{,}75i_i$ or 1,00;

I_o = sustained out-plane moment index. In the absence of more applicable data, I_o is taken as the greater of $0{,}75i_0$ or 1,00;

M_i = in-plane moment due to sustained loads, e.g., pressure and weight:

M_o = out-of-plane moment due to sustained loads, e.g., pressure and weight;

Z = sustained section modulus. Z in equations 16 and 17 is computed in this paragraph using nominal pipe dimensions less allowances;

The equation for the stress due to sustained torsional moment, St, is

$$S_t = \frac{I_t M_t}{2Z} \qquad (18)$$

Where

I_t = sustained torsional moment index. In the absence of more applicable data, I_t is taken as 1,00;

M_t = torsional moment due to sustained loads, e.g., pressure and weight;

The equation for the stress due to sustained longitudinal force, S_a, is

$$S_a = \frac{I_a F_a}{A_p} \qquad (19)$$

Where

A_p = cross-sectional area of the pipe, considering nominal pipe dimensions less allowances; see (ASME B31.3: Process Piping, 2012, s. 41)

F_a = longitudinal force due to sustained loads, e.g., pressure and weight;

I_a = sustained longitudinal force index. In the absence of more applicable data, I_a is taken as 1,00

The sustained longitudinal force, F_a, includes the sustained force due to pressure, which is $P_j A_f$ unless the piping system includes an expansion joint that is not designed to carry this force itself, where P_j is the internal operating pressure for the condition being considered, $A_f = \pi d^2/4$, and d is the pipe inside diameter considering pipe wall thickness less applicable allowances; see (ASME B31.3: Process Piping, 2012, s. 41)

4.2.2.2. Stress due to sustained loads according to EN 13480-3

The sum of primary stresses σ_1, appearing due to calculation pressure P, M_A moment resulting from weight and other sustained stresses shall fulfil the following condition:

$$\sigma_1 = \frac{PD}{4e_n} + \frac{0{,}75\, i\, M_A}{Z} \leq f_h \qquad (20)$$

Where

M_A = the resultant moment from the sustained mechanical loads which shall be determined by using the most unfavourable combination of the following loads:

1. Piping dead weight including all the internal and external attachments such as insulation, valves, lining;
2. Weight of conveyed fluid;
3. Internal pressure forces due to unrelieved axial expansion joints.

(EN 13480-3, 2012, s. 275)

4.2.3. Stress range due to thermal expansion and alternating loads according to EN 13480-3

The stress range, σ_3, due to the resultant moment, M_C, from thermal expansion and alternating loads, e.g. seismic loads, shall either satisfy the following equation:

$$\sigma_3 = \frac{iM_c}{Z} \leq f_a \qquad (21)$$

Or where the conditions of equation 21 are not met, the sum of stresses, σ_4, due to calculation pressure P, resultant moment, M_c, from thermal expansion and alternating loads shall satisfy the following equation 22:

$$\sigma_4 = \frac{PD}{4e_n} + \frac{0.75iM_A}{Z} + \frac{iM_C}{Z} \leq f_h + f_a \qquad (22)$$

Where

M_C is the range of resultant moment due to thermal expansion and alternating loads which shall be determined from the greatest difference between moments using the moduli of elasticity at the relevant temperatures.

Particular attention shall be given to:

1. Longitudinal expansion, including terminal point movements, due to thermal expansion and internal pressure;

2. Terminal point movements due to earthquake if anchor displacement effects were omitted from corresponding equation (EN 13480-3, 2012, s. 45)(not considered within the scope of this work);
3. Terminal point movements due to wind (not considered within the scope of this work);
4. Frictional forces;

(EN 13480-3, 2012, s. 277)

4.2.4. Flexibility stresses

4.2.4.1. Flexibility stress according to ASME B31.3

a) The range of bending and torsional stresses shall be computed using the reference modulus of elasticity at 21°C, Ea, and then combined in accordance with equation 23 to determine the computed displacement stress range, S_E, which shall not exceed the allowable stress range, S_A.

$$S_E = \sqrt{(|S_a + S_b|)^2 + (2S_t)^2} \qquad (23)$$

Where

A_p = cross-sectional area of pipe;

F_a = range of axial forces due to displacement strains between any two conditions being evaluated;

i_a = axial stress intensification factor. In the absence of more applicable data, i_a = 1,0 for elbows, pipe bends, and miter bends and $i_a = i_o$ (or i when listed) in (ASME B31.3: Process Piping, 2012, ss. 384-387) for other components;

i_t = torsional stress intensification factor. In the absence of more applicable data, i_t = 1,0;

M_t = torsional moment;

Sa = axial stress range due to displacement strains;

$= i_a F_a / A_p$;

S_b = resultant bending stress;

S_t = torsional stress;

$= i_t M_t / 2Z$;

Z = section modulus of pipe

b) The resultant bending stresses, S_b, to be used in equation 23 for elbows, miter bends, and full size outlet branch connections shall be calculated in accordance with equation 24, with moments as shown in (ASME B31.3: Process Piping, 2012, s. 40)

$$S_b = \frac{\sqrt{(i_i M_i)^2 + (i_o M_o)^2}}{Z} \qquad (24)$$

Where

i_i = in-plane stress intensification factor from (ASME B31.3: Process Piping, 2012, ss. 384-387);

i_o = out-plane stress intensification factor from (ASME B31.3: Process Piping, 2012, ss. 384-387);

M_i = in-plane bending moment;

M_o = out-of-plane bending moment;

S_b = resultant bending stress;

Z = section modulus of pipe;

(ASME B31.3: Process Piping, 2012, ss. 38-39)

4.2.4.2. Time-independent nominal design according to EN 13480-3

For steels other than austenitic steels design stress shall be chosen in accordance with:

$$f = min\ \left\{\frac{R_{eHt}}{1,5}\ or\ \frac{R_{p0,2t}}{1,5}\ ;\ \frac{R_m}{2,4}\right\} \qquad (25)$$

As the pipework material is A106 Grade B that is carbon steel, equation 25 is valid for this work.

(EN 13480-3, 2012, s. 41)

4.2.5. Bases for allowable stresses

Allowable stress values at design temperature for materials shall not exceed the lower of two-thirds of S_Y and two-thirds of S_{yt}. S_{yt} is determined in accordance with equation 26.

$$S_{yt} = S_Y R_Y \qquad (26)$$

Where

R_Y = ratio of the average temperature dependent trend curve value of yield strength to the room temperature yield strength;

S_Y = specified minimum yield strength at room temperature;

S_{yt} = yield strength at temperature

(ASME B31.3: Process Piping, 2012, s. 117)

4.2.6. Boundary conditions

Boundary conditions shall be imposed on the model according to the real-life support conditions, applied supports and agreed assumptions. Supports represent certain movements limitations imposed on piping either in translational or rotational directions or both. In this work boundary conditions had been imposed on the system according to the overall drawings of the system and documentation. For FEM simulation, boundary conditions had been imposed as it is shown on figure 2. Lower vessel supports are fixed on the lower plane as they are bolted to the concrete platform and assumed immovable. Top vessel has two supports with different boundary conditions. Left support's bottom face is assumed immovable as well and right support bottom is allowed only to slide along vessel centreline. In SolidWorks, right support is assumed to be sliding (pinned). Also, for the piping flexibility study, system had been simulated with edges on piping where flanges usually situated being fixed as shown on Figure 6. Normally, the edges with the flange connection are not fixed.

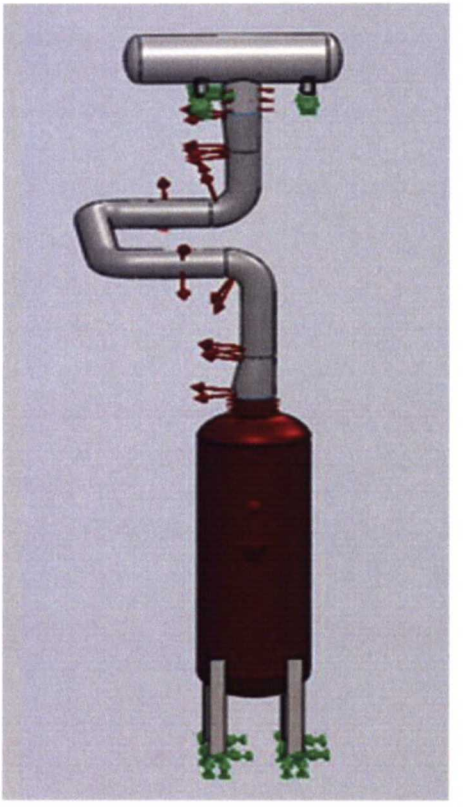

Figure 2: Boundary conditions on the SolidWorks model

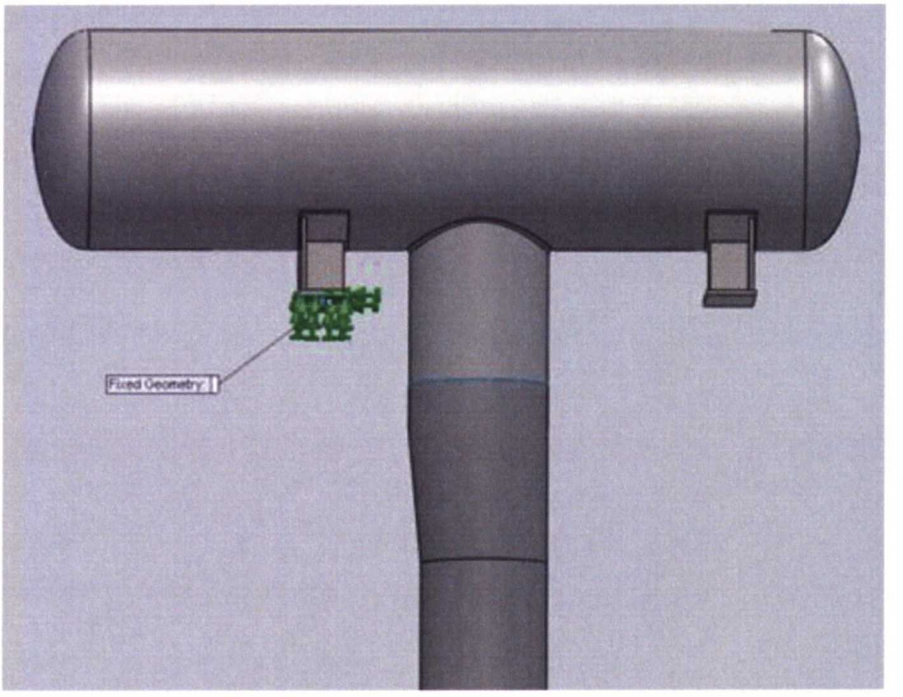

Figure 3: Fixed face on top vessel's support

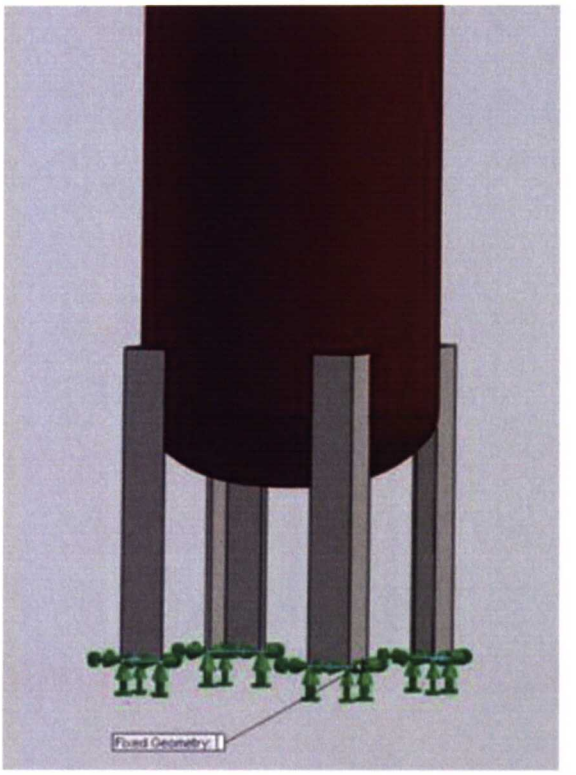

Figure 4: Fixed faces on lower vessel's supports

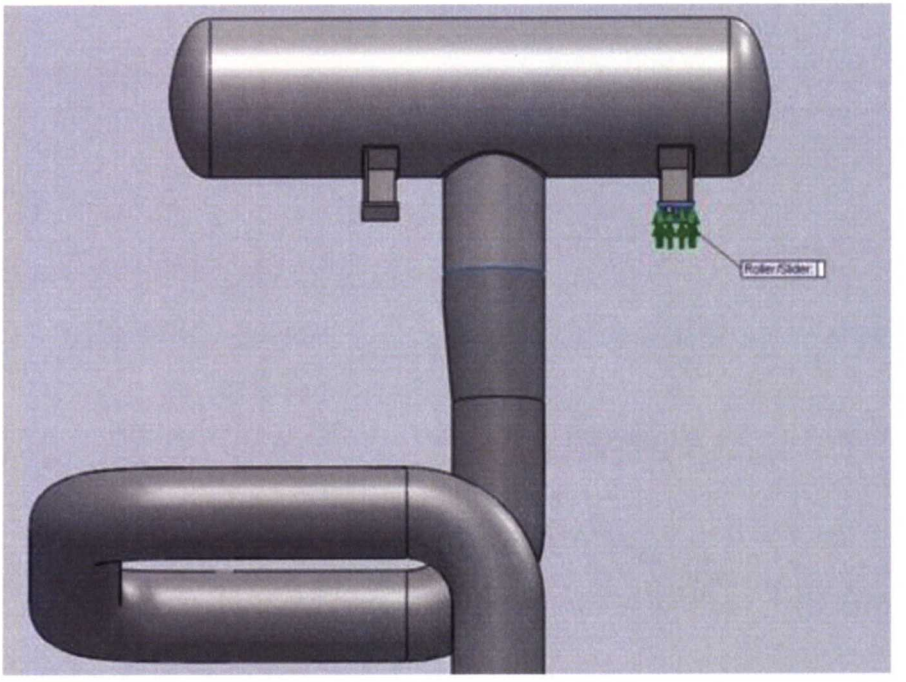

Figure 5: Sliding face of top vessel's support

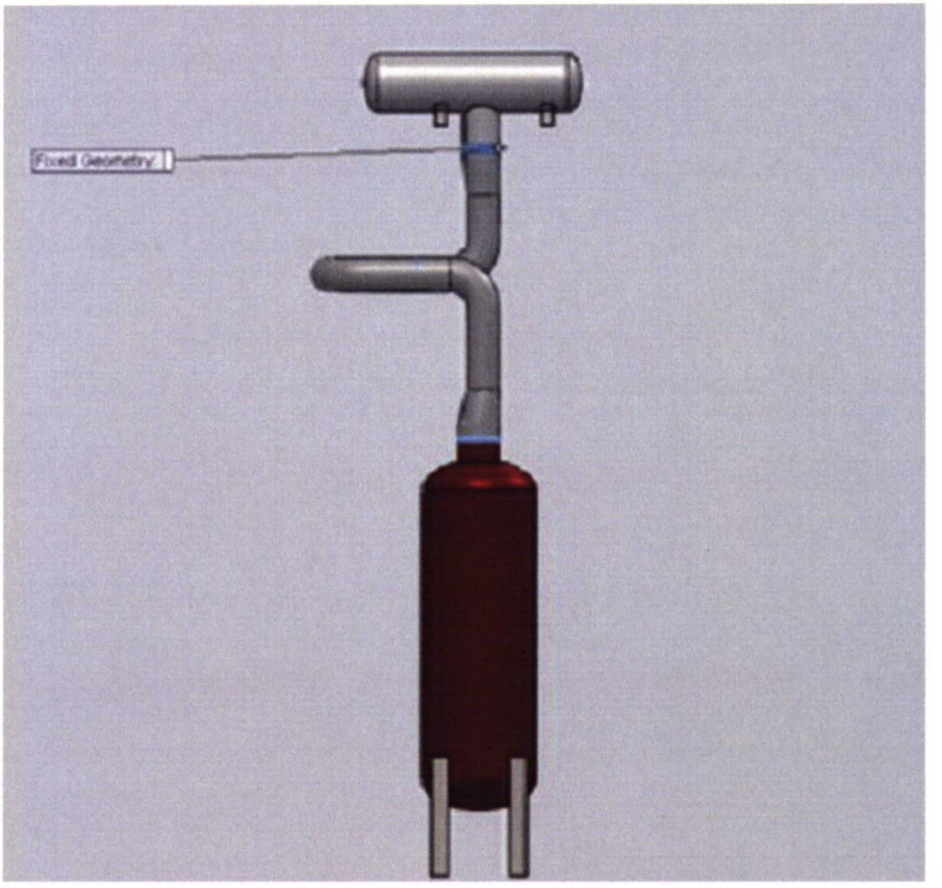

Figure 6: Fixed flange connections

4.2.7. Determination of resultant moments

In order to determine the moments, used in previously given equations, following basic principles shall be considered:

For n simultaneously applied moments M_i (i= 1,2,…,n) with the co-ordinates M_{xi}, M_{yi}, M_{zi} referred to coordinate system x,y,z that are mutually perpendicular, the total resultant moment M is the sum of the moments:

$$\vec{M} = \begin{pmatrix} M_x \\ M_y \\ M_z \end{pmatrix} = \begin{pmatrix} \sum_1^n M_{xi} \\ \sum_1^n M_{yi} \\ \sum_1^n M_{zi} \end{pmatrix} \quad (27)$$

and

$$M = \sqrt{M_x^2 + M_y^2 + M_z^2} \quad (28)$$

(EN 13480-3, 2012, ss. 279, 281, 283)

4.3. Loading conditions

Load cases that piping system is subjected have been described previously. Load acting on a system and taken into account in analysis scope shall obey the rules of (EN 13480-3, 2012, ss. 23, 25, 27). As the system analysed in this work is assumed not be subjected to dynamic, exceptional, alternating, climatic or seismic load, only following factors shall be taken into account in the simulation:

1. Internal and/or external pressure
2. Temperature
3. Weight of piping and contents

(EN 13480-3, 2012, ss. 23, 25, 27)

5. Model description

The system described above had been modelled and simulated in two types of software with different level of accuracy and conservatism. First, in CAEpipe 6.81 that is code-based software for piping stress analysis. In CAEpipe two types of modelling had been performed: first, with the maximum conservatism and applying anchors (fixed points) on nozzles and second, modelling the nozzle intersection utilizing flexibility. Secondly, FEM simulation in SolidWorks had been performed with accurate modelling of the piping, vessels and supports. Below in this section presented detailed description of models created in CAEpipe and SolidWorks and performed simulations. The research had aimed for study of nozzle reactions and flexibilities. Modelled system had been commissioned in 2007 and situated in Porvoo Refinery Area.

5.1. Modelling of the system in CAEpipe 6.81

The system had been modelled in CAEpipe 6.81 that is conventional code-base software intended for piping stress analysis. In order to build proper modelling isometric drawings of piping and overall drawings of the vessels and supports had been acquired. Original documents modelling had been based on can be found in Appendix A and B. The system allow building the models fast and check the stress level and nozzle loads with acceptable level of accuracy. In Table 5 pipe sections utilized in analysis are specified.

Section name (outside diameter in inches)	Section outside diameter, mm	Section wall thickness, mm	Insulation thickness, mm	Lining thickness, mm
12	323,85	9,53	50	0
14	355,6	9,53	50	0
16	406,4	9,53	50	0

Table 5: Pipe sections utilized in CAEpipe

Piping mechanical and physical properties of the material had been utilized in analysis are specified in table 6.

Pipe material: A106 Grade B			
Density = 7833 kg/m^3, Nu = 0.300, Joint factor =1.00, Type = Carbon Steel			
Temperature, °C	Young's modulus, MPa	Coefficient of thermal expansion, mm/mm/°C	Allowable stress, MPa
-73,33	208222	$10.17 \cdot 10^{-6}$	137,9
21,11	203395	$10.93 \cdot 10^{-6}$	137,9
93,33	198569	$11.48 \cdot 10^{-6}$	137,9
148,9	195122	$11.88 \cdot 10^{-6}$	137,9
204,4	190985	$12.28 \cdot 10^{-6}$	137,9
260	188227	$12.64 \cdot 10^{-6}$	130,7

Table 6: Piping material mechanical and physical properties

Thirdly, load cases applied on section had been specified in Table 7:

Load case	Temperature, °C	Pressure, kPa	Specific gravity with respect to water
Design maximum	250	600	0,002
Design minimum	0	0	0,002
Operating	40	168	0,002

Table 7: Load cases

After specifying the initial data, the geometric model of the system had been created, based on the isometric drawings. Details of equipment, supports and fittings are specified. In layout window anchors, flanges, nozzles, reducers, bends had been specified. Layout can be found on Figure 7.

					Layout (17)				
#	Node	Type	DX (mm)	DY (mm)	DZ (mm)	Matl	Sect	Load	Data
1	Title =								
2	Hydrotest load: Spec. gravity = 1.0, Pressure = 3000 (kPa)								
3	Pipeline P33363-A1FB, p=500 kPa, t=250 C, RVTO3 regeneration								
4	Connects equipment FA-33392 nozzle N7								
5	10	From	60150	7050	6770				Anchor
6	15				127	106	16	1	Flange
7	18	Reducer			356	106	16	1	
8	20	Bend			1347	106	12	1	
9	25	Bend		-1500		106	12	1	
10	28		-1000			106	12	1	
11	30	Bend	-1850			106	12	1	
12	35	Bend		1500		106	12	1	
13	40				760	106	12	1	
14	50	Reducer			257	106	14	1	
15	55				237	106	14	1	Flange
16	60				371	106	14	1	Anchor
17	Connects heat exchanger EA-33316 nozzle N1								

Figure 7: Layout window in CAEpipe

On the nodes 10 and 60, on the "anchor" node, thermal equipment is connected. Thus, thermal displacements shall be specified foe each node in accordance with the equipment movements. Displacements shall be calculated according to equation 29:

$$disp = L_e \cdot \beta \cdot T \qquad (29)$$

Where

L_e = length of the equipment subjected to thermal displacement, mm;

β = coefficient of thermal expansion specific for operating temperature, mm/mm/°C;

T = operating temperature, °C

Note: displacements shall be calculated for all axes where the equipment expand/shrink.

5.1.1. Allowable nozzle loads

In order for the equipment to withstand the loads, imposed with piping, kept aligned and perform correctly, the nozzle loads imposed on the system shall be below the allowable level. Equipment allowable nozzle loads had been taken from the equipment drawings. In case of missing information on the equipment drawing, allowable loads shall be calculated according to national, industry or corporative standards regarding allowable nozzle loads for equipment. Allowable nozzle loads for the system nozzles can be found in Table 8.

Nozzle, connection	Node in CAEpipe	Outside diameter, inches	Allowable force on the nozzle, F_i, kN	Allowable moment on the nozzle, M_i, kNm
1, top nozzle, gas heater	60	14"	16,38	17,64
2, lower nozzle, regeneration unit	10	16"	18,72	23,04

Table 8: Allowable nozzle loads

5.1.2. Modelling the system in CAEpipe utilizing rigid nozzle assumption

Firstly, system had been modelled with the most conservative assumption. Nozzle-vessel connection had been assumed to be rigid joint, with no flexibility. In CAEpipe, it is represented by "Anchor" model. As the both nozzles assumed to be rigid, they are represented as rigid points and don't have flexibility. However, as the piping is connected to the thermal equipment, thermal displacements are specified for all load cases. Specified displacements can be found on Figure 8. Vessels and supports had not been modelled.

Specified Displacements (2)								
Node	Type	Load	X/x (mm)	Y/y (mm)	Z/z (mm)	XX/xx (deg)	YY/yy (deg)	ZZ/zz (deg)
10	Anchor	T1			10			
		T2			1			
		T3			-1			
60	Anchor	T1	-1		-1			
		T2						
		T3						

Figure 8: Specified anchor displacements in CAEpipe

Obtained results are distinguished as follows: code compliance, anchor loads under design maximum, operating and design minimum load. Code compliance shows the stress distribution in piping point-by-point. Methodology of this stress analysis had been given previously in Methodology chapter.

Code compliance result of the rigid assumption for sustained and expansion case can be found in Table 9:

Sustained				Expansion			
Node	SL (MPa)	SH (MPa)	SL/SH	Node	SE (MPa)	SA (MPa)	SE/SA
35B	13,30	132,1	0,10	25B	98,40	331,2	0,30

Table 9: Code compliance for rigid case in CAEpipe

Resultant nozzle (anchor) loads for design maximum load case can be found in Table 10.

Node	FZ (N) (Axial)	FX (N) (Longitudinal shear)	FY (N) (Circumferential	Torque (Nm)	Circumferential moment (Nm)	Longitudinal moment (Nm)	Pass/Fail
10	-26876	28332	518	27595	11138	20401	Fail
60	17568	-28332	-518	-29071	-8164	14762	Fail

Table 10: Anchor loads under design maximum load case

Resultant nozzle (anchor) loads for operating load case can be found in Table 11.

Node	FX (N) (Longitudinal shear)	FY (N) (Circumferential Shear)	FZ (N) (Axial)	Circumferential moment (Nm)	Longitudinal moment (Nm)	Torque moment (Nm)	Pass/Fail
10	3220	237	-7163	2939	2538	2850	Pass
60	-3220	-237	-2145	1004	2045	-3526	Pass

Table 11: Anchor loads under operating load

Resultant anchor loads for design minimum load can be found in Table 12:

Node	FX (N) (Longitudinal shear)	FY (N) (Circumferential Shear)	FZ (N) (Axial)	Circumferential moment (Nm)	Longitudinal moment (Nm)	Torque moment (Nm)	Pass/Fail
10	-1428	186	-3559	1448	-830	-1732	Pass
60	1428	-186	-5749	2673	-372	1202	Pass

Table 12: Anchor loads under design minimum load

As can be seen from above, the stress requirements fulfilled well, but the nozzle load requirements failed for the design maximum load case that is the determining. Determining nozzle loads that are axial load and longitudinal moment exceed the allowable nozzle load value. Obtained results are conservative and thus overvalued due to rigid assumption.

5.1.3. Modelling the system in CAEpipe utilizing flexible nozzle assumption

Secondly, the system had been modelled nozzle flexibility. In-built "nozzle" option for nozzle-vessel junction had been applied in modelling. In the assumption is taken into account. In software axial translational, circumferential and longitudinal rotational stiffness are calculated. The stiffness values in CAEpipe are calculated automatically utilizing tabulated diagrams from WRC 297 (Mershon;Mokhtarian;Ranjan;& Rodabaugh,

1987). However, software does not allow modelling of the vessel and the supports. Thus, certain flexibility of the system had been undermined. Nevertheless, following results are the most accurate in terms of CAEpipe software. The model simulation had yielded the following results:

Based on nozzle and vessel geometry, following nozzle stiffnesses had been generated, as can be found in Table 13.

Node	Axial stiffness (N/mm)	Circumferential (Nm/deg)	Longitudinal (Nm/deg)
10	$1{,}378 \cdot 10^7$	17610,08	$1.778 \cdot 10^5$
60	$1{,}536 \cdot 10^7$	10353,69	$1.274 \cdot 10^5$

Table 13: Nozzle stiffness

Stiffness matrix generated for the system has the size of 876 elements (see Figure 9).

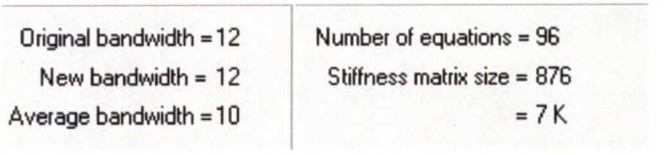

Figure 9: Stiffness matrix size

Code compliance for the nozzle modelling can be found in Table 14:

Sustained				Expansion			
Node	SL (MPa)	SH (MPa)	SL/SH	Node	SE (MPa)	SA (MPa)	SE/SA
20A	11,98	132,1	0,09	25B	79,30	328,4	0,24

Table 14: Code compliance according to nozzle modelling

The stress level had decreased slightly due to nozzle flexibility taken into account.

Results of nozzle loads can be found in Table 15, 16, 17:

Node	Axial (N)	Longitudinal load (N)	Circumferential load (N)	Torque (Nm)	Circumferential moment (Nm)	Longitudinal moment (Nm)	Pass/Fail
10	-23374	19890	907	19193	3455	9972	Failed
60	14066	-19890	-907	-21780	-1828	6004	Pass

Table 15: Design maximum load case

According to company regulations, system does not fulfil the requirements for axial load on lower nozzle.

Nozzle loads for operating case are represented as follows:

Node	Axial (N)	Longitudinal load (N)	Circumferential load (N)	Torque (Nm)	Circumferential moment (Nm)	Longitudinal moment (Nm)	Pass/Fail
10	-7003	2388	20.02.203 Guy 1110 Irina Filatova	882	795	1432	Pass
60	-2305	-2388	-1110	-4045	133	735	Pass

Table 16: Operating load case

Design minimum:

Node	Axial (N)	Longitudinal load (N)	Circumferential load (N)	Torque (Nm)	Circumferential moment (Nm)	Longitudinal moment (Nm)	Pass/Fail
10	-3766	-1069	1148	-2742	295	-250	Pass
60	-5542	1069	-1148	-530	501	-303	Pass

Table 17: Design minimum load on nozzles

5.1.4. Comparison between results obtained for rigid and flexible assumptions in CAEpipe

As the flexibility of the nozzle had been introduced to the simulation, the loads had decreased for the flexible simulation case. First, the stress level decreased can be seen from Table 18.

Difference from changing the model from rigid to partly-flexible (nozzle assumption), %					
Code compliance					
Sustained			Expansion		
SL (Mpa)	SH (Mpa)	SL/SH	SE (Mpa)	SA (Mpa)	SE/SA
-10	0	-10	-19,4	-0,8	-20

Table 18: Comparison between the rigid and flexible assumption in CAEpipe

Also, the nozzle reactions had decreased more significantly due to the nozzle flexibility introduction. The difference can be found from Tables 19-21.

Difference from changing the model from rigid to partly-flexible, %						
Maximum design load						
Node	Longitudinal shear	Circumferential Shear	Axial	Circumferential Moment	Longitudinal moment	Torque
10	-13	-29,7	77,6	-30,4	-69	-50,9
60	-20	-29,7	77,6	-24,9	-77.1	-58,9

Table 19: Comparison between the nozzle reactions for rigid and flexible assumption for maximum design load

Difference from changing the model from rigid to partly-flexible, %						
Operating case						
Node	FX (N) (Axial)	FY (N) Longitudinal shear	FZ (N) Circumferential shear	Torque (Nm)	Circumferential moment (Nm)	Longitudinal moment (Nm)
10	-2,2	-25,7	367,9	-68,9	-73	-43,4
60	7,5	-25,7	367,9	14,7	-86,4	-63,6

Table 20: Comparison between the nozzle reactions for rigid and flexible assumption for maximum design load

Difference from changing the model from rigid to partly-flexible, %						
Design minimum case						
Node	FX (N) (Axial)	FY (N) Longitudinal shear	FZ (N) Circumferential shear	Torque (Nm)	Circumferential moment (Nm)	Longitudinal moment (Nm)
10	5,8	-25,1	517,2	58,3	-79,6	-69,9
60	-3,6	-25,1	517,2	-55,9	-81,3	-18,5

Table 21: Comparison between the nozzle reactions for rigid and flexible assumption for maximum design load

Case with maximum rigidity would fail the design requirements as the nozzle loads exceed the allowable values. However, the introduction of the flexibility of the nozzles does not give the even decrease of all nozzle load values. Axial force got increased for the design maximum load case but decreased on node 10 for the operating load and on node 60 on the design minimum load case. Longitudinal and circumferential moments significantly decreased for all design cases.

5.1.5. Nozzle flexibility factors calculations based on CAEpipe results

Flexibility calculation based on results obtained from CAEpipe can be found from Appendix D. Calculations had been based on WRC bulletin guidelines and performed for all load cases. The yielded results are axial translational, circumferential and longitudinal rotational nozzle flexibility. Nozzle flexibility factor is the ratio of the rotation per unit length of the part in question produced by a moment, to the rotation per unit

length of a straight pipe of the same nominal size and schedule or weight produced by the same moment. (Markl, 1955, s. 1955)

5.1.6. Conclusions

Nozzle load resulting from rigidity assumption and nozzle load resulting from flexibility assumption differ significantly. Nozzle load emerging in maximum design load does not meet the requirement of allowable load. Both vessels types are pressure vessels. So, significant characteristics such as axial load, circumferential and longitudinal loads differ for rigid and partly flexible assumption and the entity justifies the further development of model with comprehensive flexibility.

5.2. Modelling in SolidWorks software

Model of the pipeline system had been created and simulated in SolidWorks. FEM model of the system had been designed with maximum accuracy in material and loading but the system structure had been simplified where needed. For example, flanges had not been modelled to simplify the calculation stage. Bottom faces of the lower vessel supports had been modelled as fixed points. Piping, vessels and nozzles had been modelled as shells, with behaviour following thin shell theory. Supports had been modelled as solid elements.

Shell modelling had contributed the model to be simpler and simulation run faster. As the model is rather complex, the system shall be simplified as much as possible. The insulation had not been included to the modelling and simulation in order to simplify the model and to approach the maximum accurate results. The materials had been assigned to corresponding parts. Material model of the system is described in para. 1.4.1. The material temperature-dependent data had been acquired from corresponding standards.

For nozzle flexibility research boundary conditions had been imposed in accordance with the equipment drawings. The lower parts of the gas heater supports are bolted to the concrete, thus in model they are fixed points. On the top vessel left-hand side support's lower face is bolted to the supporting steel structure, thus in model the lower face is fixed part. Top vessel's support's lower face is a sliding part according to original drawing, thus in model the lower face is pinned, the face is allowed to move along the vessel's centreline; in other directions the face is fixed. In order to perform additional study of influence of the intermediate constraints, two cases had been examined: with both flange connections fixed and with lower flange connection fixed, while the top flange connected was free to rotate. However, connections had stayed free for thermal displacement.

The model had been simulated for three load cases (see Table 22) found from the pipeline specifications and equipment drawings.

	Temperature, °C			Pressure, kPa		
	Design max	Design min	Operating	Design max	Design min	Operating
Piping	250	0	40	600	0	168
Lower Vessel	250	0	40	500	0	160
Top Vessel	285	0	70	500	0	80

Table 22: Loads on piping

Overall system drawings model is shown on Figures 10-11. More detailed drawings can be found in Appendix C.

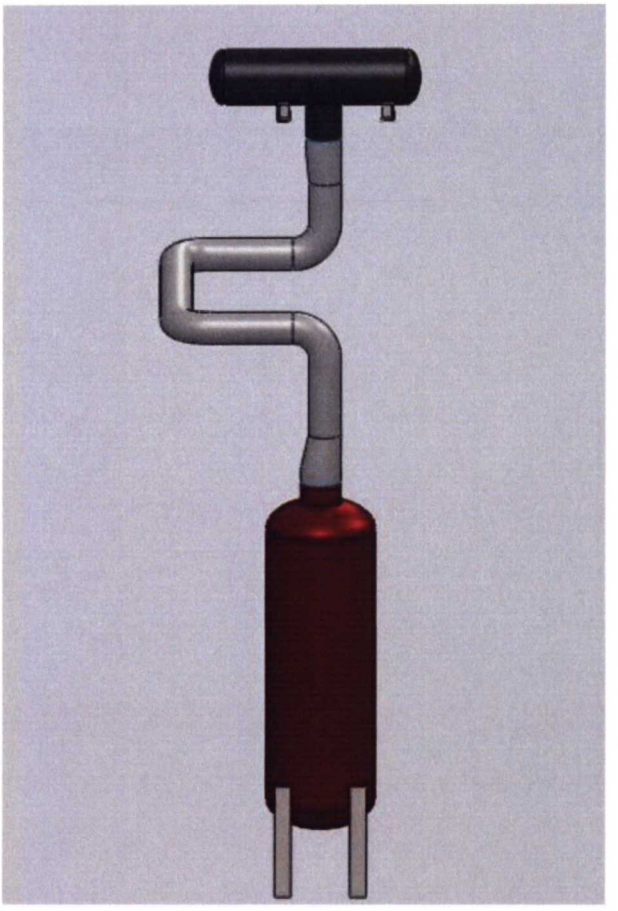

Figure 10: SolidWorks model front view

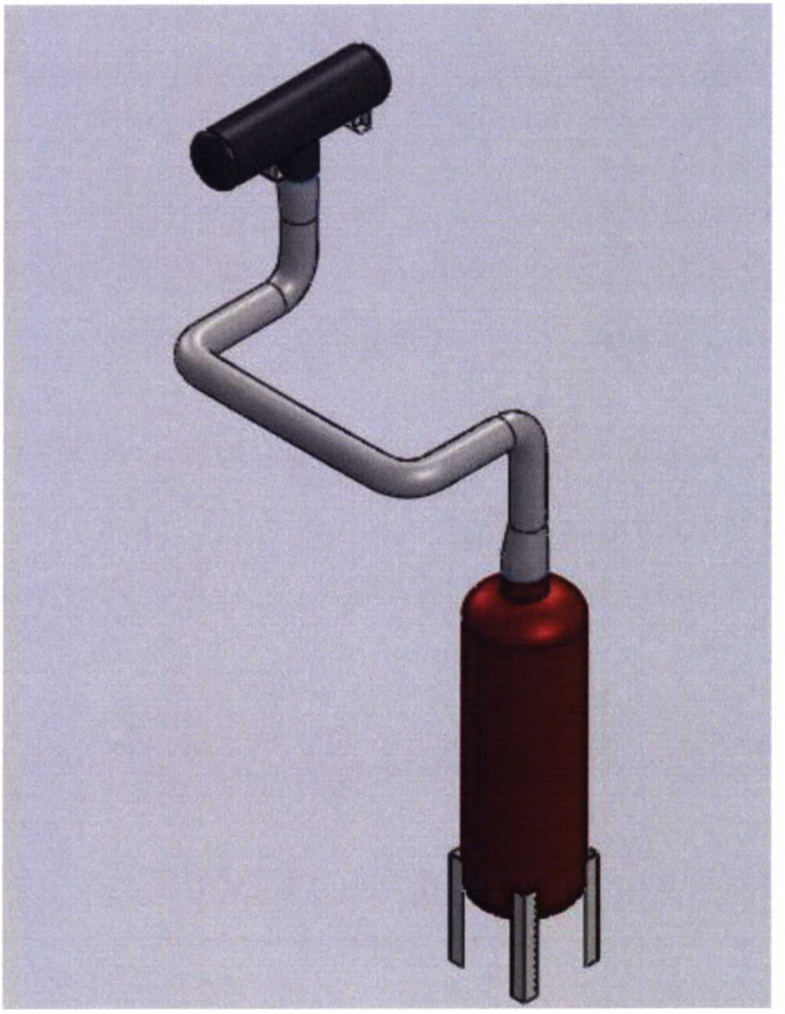

Figure 11: SolidWorks model isometric view

5.3. Results obtained from SolidWorks simulation

Nozzle loads obtained for three load cases from SolidWorks simulation are as follows:

Nozzle reactions for design maximum load case for the flexible nozzles can be found in Table 23.

	Axial force, N	Circumferential moment, Nm	Longitudinal moment, Nm
Lower nozzle	27,05	-0,015	-0,0062
Top nozzle	-11,17	0,16	0,018

Table 23: Results for maximum design load case in SolidWorks

Nozzle reaction for operating load case for flexible nozzles can be found in Table 24.

	Axial force, N	Circumferential moment, Nm	Longitudinal moment, Nm
Lower nozzle	27,04	-0,015	-0,0063
Top nozzle	-10,99	0,16	0,018

Table 24: Results for operating load case in SolidWorks

Nozzle reaction for design minimum load case for flexible nozzles can be found in Table 25.

	Axial force, N	Circumferential moment, Nm	Longitudinal moment, Nm
Lower nozzle	465,17	-0,26	-0,11
Top nozzle	-188,65	2,73	0,30

Table 25: Results for minimum design load case

Results for nozzle displacement and rotation are as follows:

Rotation and displacement for design maximum load case can be found in table 26.

	Axial displacement, mm	Circumferential rotation, rad	Longitudinal rotation, rad
Lower nozzle	0,16	-0,000011	-0,0000093
Top nozzle	-0,042	-0,000047	-0,000012

Table 26: Results for maximum design load case in SolidWorks

Results for nozzle displacement and rotation for operating load case with flexible nozzles can be found in Table 27.

	Axial displacement, mm	Circumferential rotation, rad	Longitudinal rotation, rad
Lower nozzle	-0,027	0,0000026	-0,0000031
Top nozzle	-0,027	-0,000017	-0,00001

Table 27: Results for operating load case in SolidWorks

Results for nozzle displacement and rotation for design minimum load case can be found in Table 28.

	Axial displacement, mm	Circumferential rotation, rad	Longitudinal rotation, rad
Lower nozzle	-2,85	0,00015	-0,00014
Top nozzle	-0,12	-0,000038	-0,000066

Table 28: Results for design minimum case in SolidWorks

Reactions on nozzle-vessel intersection for the simulation with both boundary conditions with two flange connections fixed are as follows.

Reaction loads and moments on design maximum load case with fixed flanges can be found in Table 29.

	Axial force, N	Circumferential moment, Nm	Longitudinal moment, Nm
Lower nozzle	27,07	-0,015	-0,0061
Top nozzle	-11,16	0,16	0,018

Table 29: Results for maximum design load case with fixed flanges in SolidWorks

Nozzle reactions for operating load case with fixed flanges can be found in table 30.

	Axial force, N	Circumferential moment, Nm	Longitudinal moment, Nm
Lower nozzle	27,03	-0,015	-0,0063
Top nozzle	-11,01	0,16	0,018

Table 30: Results for operating load with fixed flanges case in SolidWorks

Nozzle reactions for design minimum load case with fixed flanges can be found in table 31.

	Axial force, N	Circumferential moment, Nm	Longitudinal moment, Nm
Lower nozzle	465,27	-0,25	-0,11
Top nozzle	-188,75	2,73	0,30

Table 31: Results for design minimum load case with fixed flanges in SolidWorks

Displacements and rotations on the nozzles for design maximum load for fixed flanges modelling can be found in Tables 32-34.

	Axial displacement, mm	Circumferential rotation, rad	Longitudinal rotation, rad
Lower nozzle	0,013	-0,00000095	0,0000017
Top nozzle	-0,014	-0,0000021	-0,00003

Table 32: Results for maximum design load case with fixed flanges in SolidWorks

	Axial displacement, mm	Circumferential rotation, rad	Longitudinal rotation, rad
Lower nozzle	-0,0068	0,00000068	-0,0000036
Top nozzle	-0,016	-0,00000043	-0,000022

Table 33: Results for operating load case with fixed flanges in SolidWorks

	Axial displacement, mm	Circumferential rotation, rad	Longitudinal rotation, rad
Lower nozzle	-2,85	0,00015	-0,00014
Top nozzle	-0,12	-0,000039	-0,000015

Table 34: Results for design minimum case with fixed flanges in SolidWorks

As can be seen from above tables, the reactions on the nozzles haven't changed significantly with the alternation of the boundary conditions, but difference for

displacements and rotation is substantial, that influences on the flexibility factors (see Appendix D).

6. Analysis of results

Difference between the CAEpipe simulation results and FEM simulation results is significant. The complete pivot tables can be found in Appendix E. Simulation of different boundary conditions in FEM yielded various results for the cases of flanges not fixed and case with flanges fixed due to the inability of the area to move freely. Reaction load on the junction for the free flanges and flanges fixed is practically equal but fixed flanges have displacements exceeding free flange value. For the cases of both flanges fixed and only lower flange fixed difference is in top nozzle displacement. Thus, yielded flexibility factors differ for various cases of boundary conditions. Highest flexibility had been yielded for the FEM model with no additional fixtures. Relatively high values of flexibility factors for the CAEpipe modelling results are explained with the use of WRC 297 values for stiffness coefficient calculation. The coefficients are intended for the vessels with no pressure applied. Research showed that applied pressure decrease the flexibility of the nozzle. (Moore;Rodabaugh;Mokhtarian;& Gwaltney, 1987, ss. 75-77).

As can be seen from the results of the nozzle load comparison, the difference between the different methods of calculation is large. Highest nozzle load values are recognized in CAEpipe analysis in rigid assumption case under design maximum load. The axial force reaction values under design load case achieve values, exceeding the allowable values. Axial load on nozzle 1 exceeds allowable load on 7.3% and axial load for nozzle 2 exceeds allowable load on 43.6%. The exaggerated values for reaction load had been caused by the rigid assumption for nozzles. Thermal movements appearing on an adjacent areas to the nozzle, cannot freely expand or shrink due to the fixed boundary condition on nozzle and thus cause the overstress. Flexibility of the vessels and supports is also not taken into account.

Second highest results have been obtained for simulation in CAEpipe with flexible assumption case. Results for the nozzle 1 are below allowable loads in maximum design case. For nozzle 2 the axial force exceeds the allowable level on 24,9%, but the circumferential and longitudinal moments are well below the allowable moment level. Axial force is rather high due to the software limitation for nozzles. It is not possible to create the nozzle, laying on the same axis with the connecting pipeline. Thus, the lower nozzle model is not accurate and its reaction loads are distorted, especially the axial force is susceptible because the vessel's orientation cannot be modelled properly in CAEpipe.

Third highest reactions had been obtained in FEM simulation with flange connections fixed. The nozzle forces and moments do not differ significantly from the FEM simulation results with flanges not fixed. Nevertheless, nozzle axial displacement,

circumferential and longitudinal rotations are considerably lower for the fixed flange case that decreases the flexibility factor value for the corresponding case.

Lowest results have been achieved in FEM simulation in SolidWorks. The modelling had been performed in maximum accurate fashion. Yielded results had shown the significant difference between the allowable nozzle loads and real loads. Greatest difference between the allowable load and real load had been obtained for longitudinal moment. That fact puts under question the existing rules for determining the allowable nozzle loads. Comprehensive FEM modelling and simulation had shown that the difference between assumed allowable and assumed real results is enormous. Particularly it is noticeable as the benchmark for the decision making is design load case. Design load is the most severe load combination that is approved based on PID in process group. Under normal working circumstances neither maximum nor minimum design load case can be achieved. Operating load is a normal working condition. If the allowable nozzle load and results for FEM simulations will be compared for design maximum and operating load case, comparison can be found in Table 35. Comparison charts on Figures 12-15 can show the scale of the difference between allowable nozzle loads and values obtained in FEM simulation.

Nozzle flexibility factor calculation can be found in Appendix D. The calculation had been based on guideline given in (Mershon;Mokhtarian;Ranjan;& Rodabaugh, 1987, ss. 69-71). Comparison of the nozzle flexibility factors obtained for FEM simulation can be found in Appendix D.5. As can be seen from figures 20-21, highest flexibility factors are typical for the design load with minimum pressure (in these particular cases acting pressure is equal zero, in fact that is no acting pressure). Lowest flexibility factors are typical for design load with maximum acting pressure. These results prove the theory from (Moore;Rodabaugh;Mokhtarian;& Gwaltney, 1987) concerning decreasing of the nozzle flexibility with increasing the acting pressure. Therefore, structures subjected to pressure load possess lower flexibility than the structures not subjected to pressure load as well as the structures; subjected to higher pressure value, possess lower flexibility than structures subjected to lower pressure value. All considered flexibilities that are axial translational, circumferential translational and longitudinal rotational, fall within this regularity in case of FEM simulation with no intermediate restraints. Accordingly, structures subjected to high pressure possess minimum flexibility.

	Axial force, kN		Share of the load, based on allowable load, %	Circumferential moment, kNm		Share of the load, based on allowable load, %	Longitudinal moment, kNm		Share of the load, based on allowable load, %
	Allowable	FEM		Allowable	FEM		Allowable	FEM	
esign num load zzle 1	16,38	-0,011	0,07	17,64	- 0,00016	0,001	17,64	0,000018	0,0001
zzle 2	18,72	0,027	0,1	23,04	-1,6E-05	0,00007	23,04	-1,8E-05	0,00008
ting load zzle 1	16,38	-0,011	0,07	17,64	0,00016	0,001	17,64	0,000018	0,0001
zzle 2	18,72	0,027	0,1	23,04	-1,5E-05	0,00007	23,04	-6,3E-06	0,00003

Table 35: Comparison of the allowable nozzle loads with results obtained from FEM simulation.

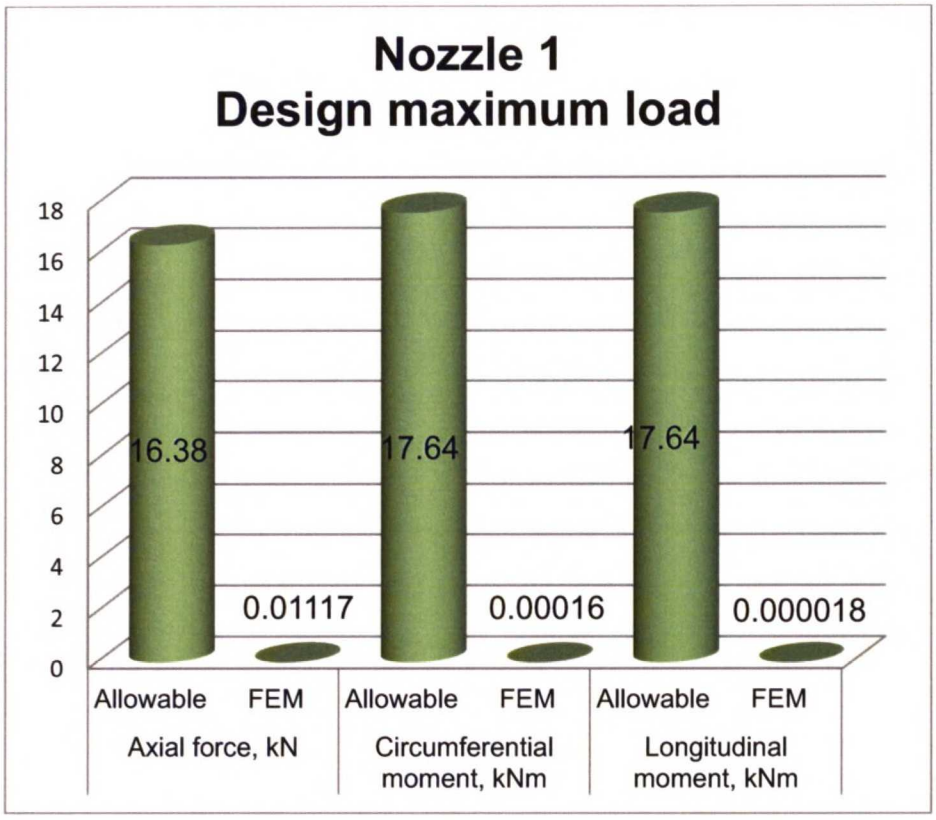

Figure 12: Comparison of loads for nozzle 1 under design maximum load

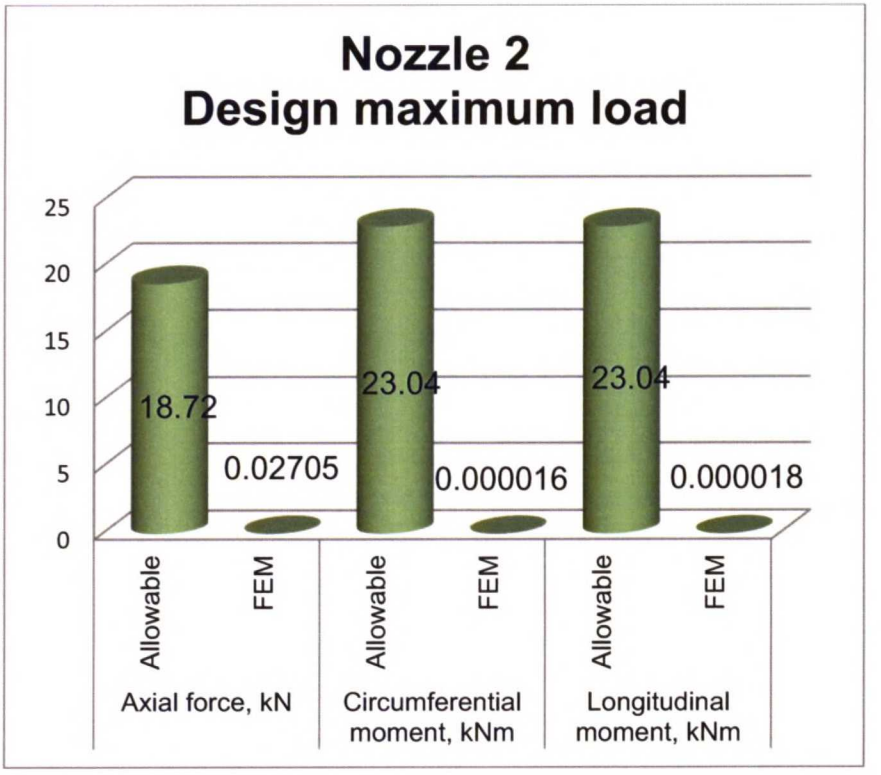

Figure 13: Comparison of loads for nozzle 2 under design maximum load

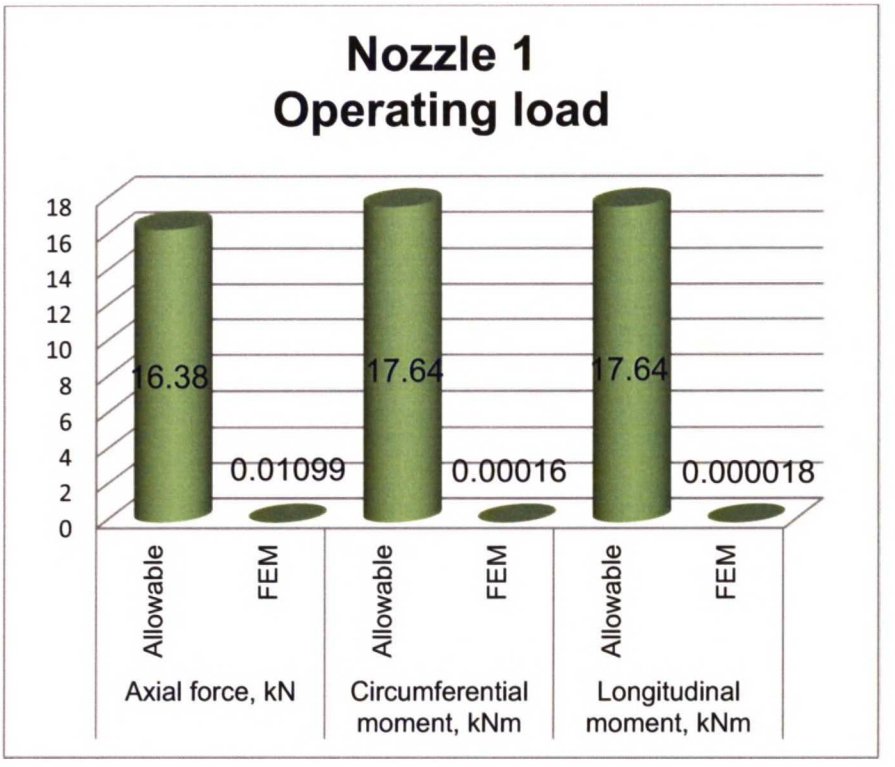

Figure 14: Comparison of loads for nozzle 1 under operating load

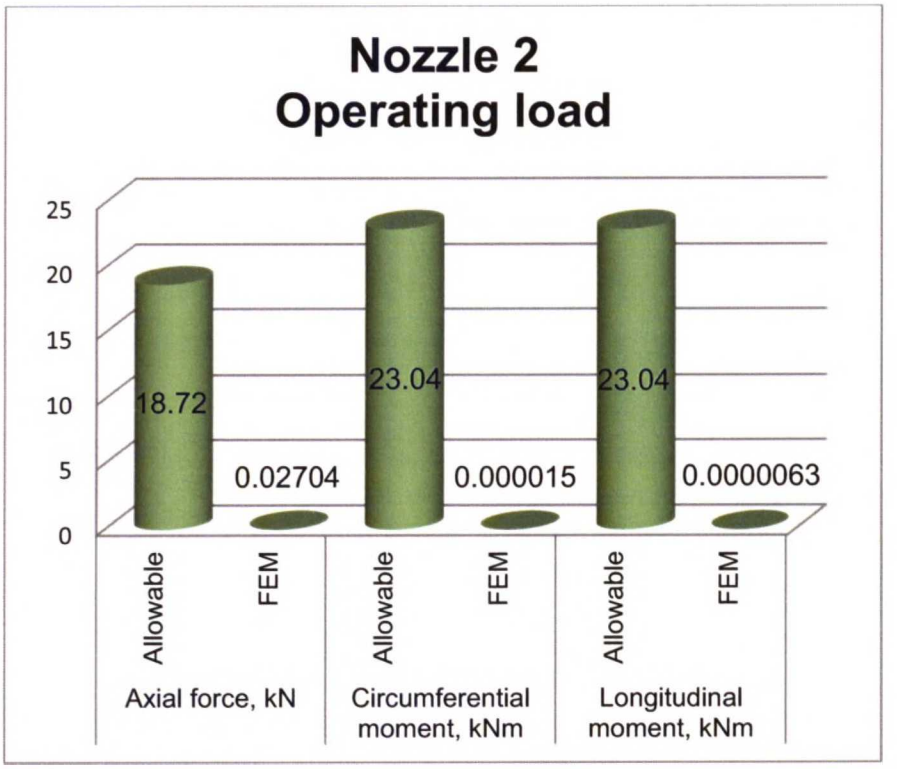

Figure 15: Comparison of loads for nozzle 2 under operating load

Reactions only for design maximum and operating load cases had been compared as the design minimum load case is less critical and rarely can be utilized as the benchmark loading.

7. Discussion

Nozzle reaction forces and moments for the different modelling types and for different boundary conditions had been obtained and compared. Flexibility factors had been calculated and compared for different models. As it was expected, highest inherent flexibility is possessed by FEM model with no intermediate constraints. The model is the most similar to real model, thus the results are assumed to be trusted.

As can be seen from Table 36, highest flexibility factors (corresponding to the lowest value in the table) in most cases are found for FEM simulation results with no intermediate constraints. Second highest flexibility can be observed in FEM model with intermediate constraint on flange connections. Third highest flexibility is distinctive for CAEpipe with nozzle modelling. Lowest results are obtained for the CAEpipe simulation with rigid nozzles. Significant difference between results for FEM simulation and CAEpipe simulation, also with nozzle modelling is explained by not taking into account vessel and supports flexibility in CAEpipe modelling. All simulation results had been compared to (Mershon;Mokhtarian;Ranjan;& Rodabaugh, 1987, ss. 62-63) Table 59-60 values for corresponding geometries. Significant difference between flexibility factors for

FEM modelling and WRC 297 table values can be explained the insufficient information in WRC 297 tables that can be applicable only for the geometry specified in the Figures 59-60 (Λ, λ) and non-linear and three-argument dependent nature of the curves that makes interpolation problematic. Due to the fact that in WRC 297 stiffness coefficients had been obtained for the structures not subjected to pressure, utilizing of the WRC 297 stiffness coefficients in CAEpipe modelling of piping system subjected to pressure gives distorted results. According to (Moore;Rodabaugh;Mokhtarian;& Gwaltney, 1987), system subjected to pressure, possesses lower inherent flexibility. Therefore, the results such as reaction load, displacements, rotations and calculated flexibility factors are most accurate for the FEM modelling with no intermediate constraints. However, it can be more time-consuming and costly to utilize FEM modelling of the whole system for checking the nozzle load level in piping design. Therefore, design specifications and rules for piping and pressure vessel design can be reviewed. Pressure vessel nozzles allowable load level can be reduced and benchmark for the piping design can be utilize the lower combination of pressure and temperature combination load case than for maximum design load case due to extremely low probability of the appearance of such load case in practice.

8. Conclusions

The goal of this work included studying the piping stress analysis methodology and learning the flexibility factors calculation methods. Literature research of the present state of art of nozzle flexibility factors calculation had been performed and revealed the character of preceding research had been performed mostly for the partial models not subjected to pressure that would give erroneous nozzle flexibility factors values for the nozzles in piping systems subjected to pressure. Vessels, intermediate and vessel supports introduce the flexibility to the piping system and nozzle. Background for modern piping stress analysis had been studied.

In order to achieve the goals of the work, structural model had been created and simulated in CAEpipe 6.81, code-based piping stress analysis software. Comprehensive structural and FEM model had been built and simulated in SolidWorks. Results of the nozzle loads obtained from simulation conducted in CAEpipe and SolidWorks had been compared to the allowable nozzle loads. Based on the obtained nozzle loads and displacements, nozzle flexibility factors had been calculated according to guidelines of (Mershon;Mokhtarian;Ranjan;& Rodabaugh, 1987). Nozzle flexibility factors had been calculated for the models with different boundary conditions and compared. The benchmark of the research had been FEM model of piping without intermediate restraints. As the model had been modelled with maximum accuracy, obtained results are sufficiently accurate and can be applied in future research of nozzle flexibility.

This work had been a background for reviewing the existing piping design specification and piping stress analysis guideline. Next phase of the work is the development of the guideline for piping stress analysis of the new format. Obtained results for the nozzle loads represent a base for the following redaction of the piping design specification. Due to the significant difference between allowable nozzle loads and FEM results for the maximum design case, rules concerning determination of allowable nozzle loads shall be reviewed. According this work's results of simulation of the FEM model, difference between design maximum and operating nozzle loads is substantial, that makes possible editing the piping design rules.

Analysis of the obtained results had shown that nozzle flexibility factors shall be used in piping stress analysis as they allow assessing the stress level on the nozzles and other connections with higher accuracy. Even with conservative Code-based software such as CAEpipe utilizing the flexibility factors into the piping stress analysis allow obtaining more accurate results of the nozzle load.

Obtained results of this work justify the implementation of the utilization of FEM modelling and analysis of the most critical lines in order to save resources and obtain accurate results. In case of FEM modelling of the most loaded lines, almost certainly lower nozzle loads can be expected that will allow piping design to utilize the maximum design capacity of the nozzles and vessels. Therefore, goals for this work had been fulfilled and the obtained results had given the background for development of the guideline for piping stress analysis.

Bibliography

A. Hardik, N. A., & Trivedi, B. R. (2011). *Stress Analysis of Reactor Nozzle to Head.* Ahmedabad: Institute of Technology, Nirma University.

American Society of Mechanical Engineers. (2012). ASME B31.3: Process Piping. New York: American Society of Mechanical Engineers.

Animated Tutorials. (2013). Retrieved from Intergraph CADWorx and Analysis Solutions: http://www.coade.com/animated_tutorials.shtml

Antaki, G. A. (2003). *Piping and Pipeline Engineering: Design, Construction, Maintenance, Integrity, and Repair.* New York: Marcel Dekker, Inc.

Bijlaard, P. P. (1954). *Stresses From Local Loadings in Cylindrical Pressure Vessels.* Ithaca, N.Y.: Americal Society of Mechanical Engineers.

Bijlaard, P. P. (1961). *Plastic Buckling of Cylindrical Shells for Cases of Non-Homogeneous Stress Distribution.* Arlington 12, Virginia: Armed Services Technical Information Agency.

Chandramouli, P. N. (2013). Fundamentals of Strength of Materials. Delhi: PHI Learning Private Limited.

Chao, Y. J., & Yeh, S. J. (1986). Stress Concentration and Flexibility Factor of Nozzles in Ellipsoidal Pressure Vessel Heads Subject to External Moment. *International Journal of Pressure Vessels and Piping*, 1-22.

Chao, Y. J., Wu, B. C., & Sutton, M. A. (1985). Radial Flexibility of Welded-pad Reinforced Nozzles in Ellipsoidal Pressure Vessel Heads. *International Journal of Pressure Vessels and Piping*, 189-207.

Cranch, E. T. (1960). *An Experimental Investigation of Stresses in the Neighborhood of Attachments to a Cylindrical Shell.* New York: Welding Research Bulletin 60.

EN 13480-3. (2012). *Metallic industrial piping. Part 3: Design and calculation.* Brussels: European Committee for Standardization.

European Gas Pipeline Incident Data Group. (2011). *8th report of the european gas pipeline incident data group.*

Grinnell Company, Inc. (1967). Expansion and Stresses. In I. Grinnell Company, *Piping Design and Engineering* (pp. 1-65). Providence, Rhode Island: Grinnell COmpany, Inc.

Holmes, E.; Rodger, C. D.; Halligan, B. D.; Westerman, V.; Lander, D. W.; Madden, J.; Masters, E. H.;. (1973). Simplified Methods of Analysing a Pipework System. In *Handbook of Industrial Pipework Engineering* (pp. 259-263). London: McGraw-Hill Book Company (UK) Limited.

Intergraph CADWorx and Analysis Solutions. (2007, 09 18). Version 5.10 User CAESAR II User Guide. Houston, Texas, USA.

King, R. C. (1967). Expansion and Flexibility. In R. C. King, *Piping Handbook* (pp. 4-1 - 4-130). New York: McGraw-Hill Book Company.

Lanza, G. (1973). Strength of materials. New York: Gordon and Breach.

Markl, A. R. (1955). *Piping Flexibility Analysis.* New York: American Society of Mechanical Engineers.

Mershon, J. L., Mokhtarian, K., Ranjan, G. V., & Rodabaugh, E. C. (1987). *Local stresses in Cylindrical Shells Due to External Loadings on Nozzles - supplement to WRC Bulletin No. 107 (Revision I).* New York: Welding Research Council Bulletin.

Moore, S. E., Rodabaugh, E. C., Mokhtarian, K., & Gwaltney, R. C. (1987). *Review and evaluation of design analysis methods for calculating flexibility of nozzles and branch connections.* Oak Ridge: Oak Ridge National Laboratory.

Murad, F. P., & Sun, B. C. (1984). On Radial and Rotational Spring Constants of Piping-Nozzles. *5th International Conference on Pressure Vessel Technology* (p. Volume 1). New York: American Society of Mechanical Engineers.

Osage, D. A., Straub, M., Buchheim, M. E., Amos, D. E., Chiasson, T. N., & Samodel, D. (2010). *Precision Equations and Enhanced Diagrams For Local Stresses In Spherical and Cylindrical Shells Due To External Loadings For Implementation of WRC Bulletin 107 Bulletin 537.* New York: Welding Research Council Bulletin.

Schwarz, M. M. (2004). Flexibility Analysis of the Vessel-Piping Interface. *International Journal of Pressure Vessels and Piping*, 181-189.

SST Systems, Inc. (2012). *CAEpipe tutorial.* Retrieved from SST Systems, Inc.: http://www.caepipe.net/filemgmt_data/files/Tutorial_1.pdf

Steele, C. R., & Steele, M. L. (1983). Stress analysis of nozzles in Cylindrical Vessels with External load. *Journal of pressure vessel technology*, 191-200.

Steele, C. R., Steele, M. L., & Khathlan, A. (1986). An Efficient Computational Approach for a Large Opening in a Cylindrical Vessel. *Journal of Pressure Vessel Technology*, 436-442.

The M.W. Kellogg Company. (1955). Simplified Method for Flexibility Analysis. In *Design of Piping Systems* (pp. 92-93). New York: John Wiley & Sons, Inc.

Weiss, E., & Joost, H. (1997). Local and Global Flexibility of Nozzle-to-Vessel Intersections Under Local Loads as Boundary Conditions for Piping System Design. *International Journal of Pressure Vessels and Piping*, 241-247.

Appendix A: Simplified CAEpipe model with rigid nozzles

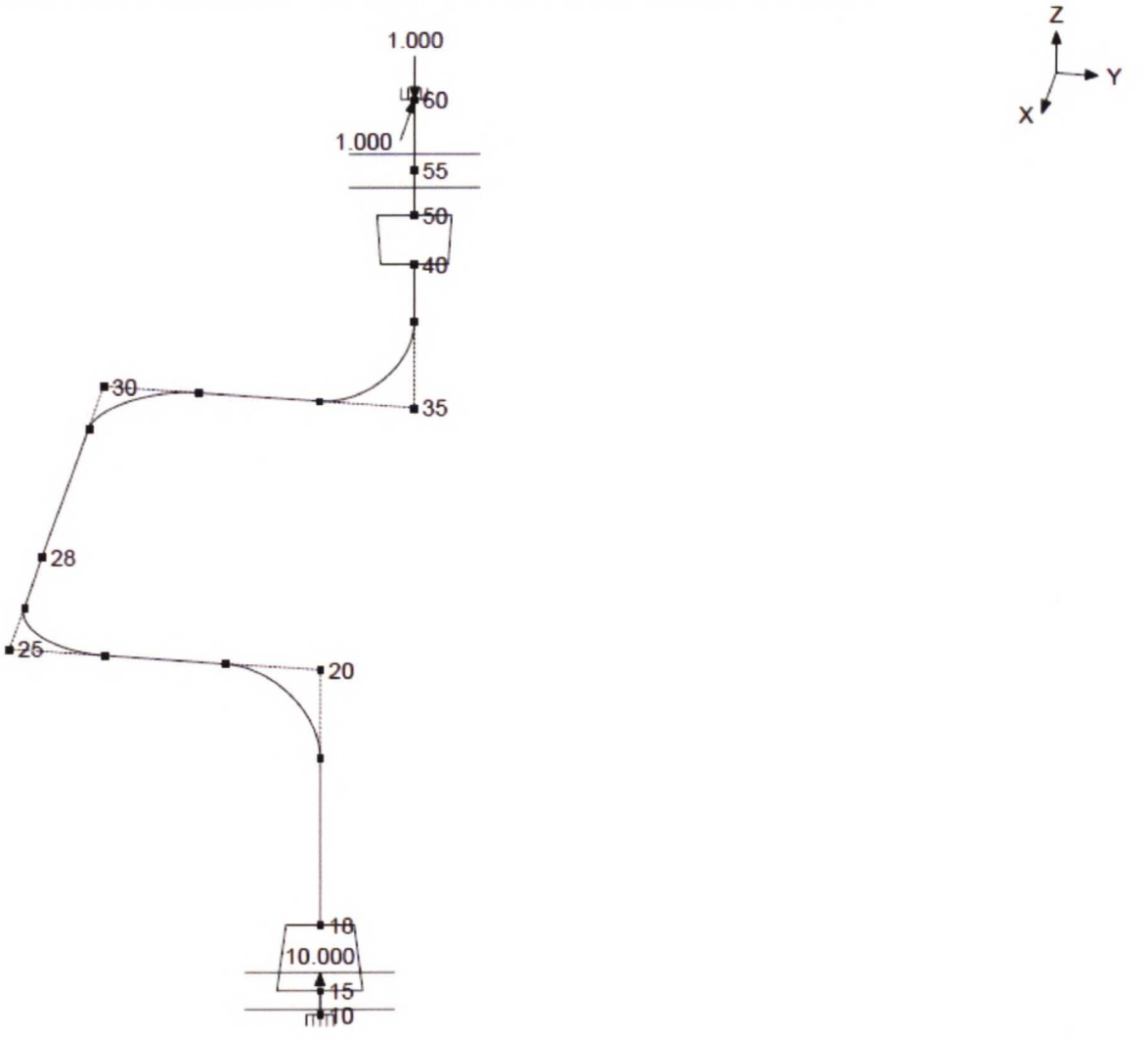

Figure 16: Simplified CAEpipe model with nozzles modelled as fixed elements. In-built element "anchor" had been utilized

Appendix B: CAEpipe model with flexible nozzle modelling

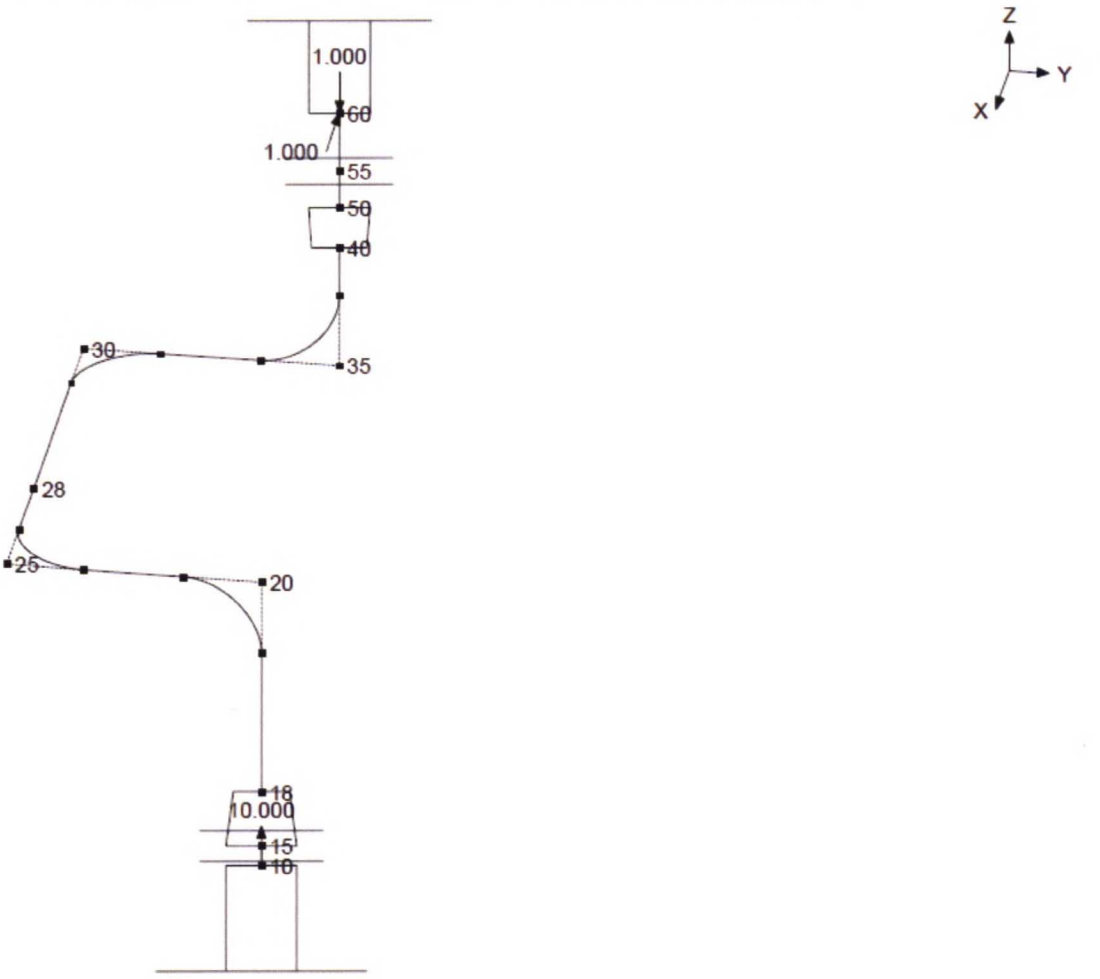

Figure 17: CAEpipe model with nozzles modeled utilizing the flexibility factors. In-built element "nozzle" had been utilized

Appendix C: SolidWorks model of the piping system

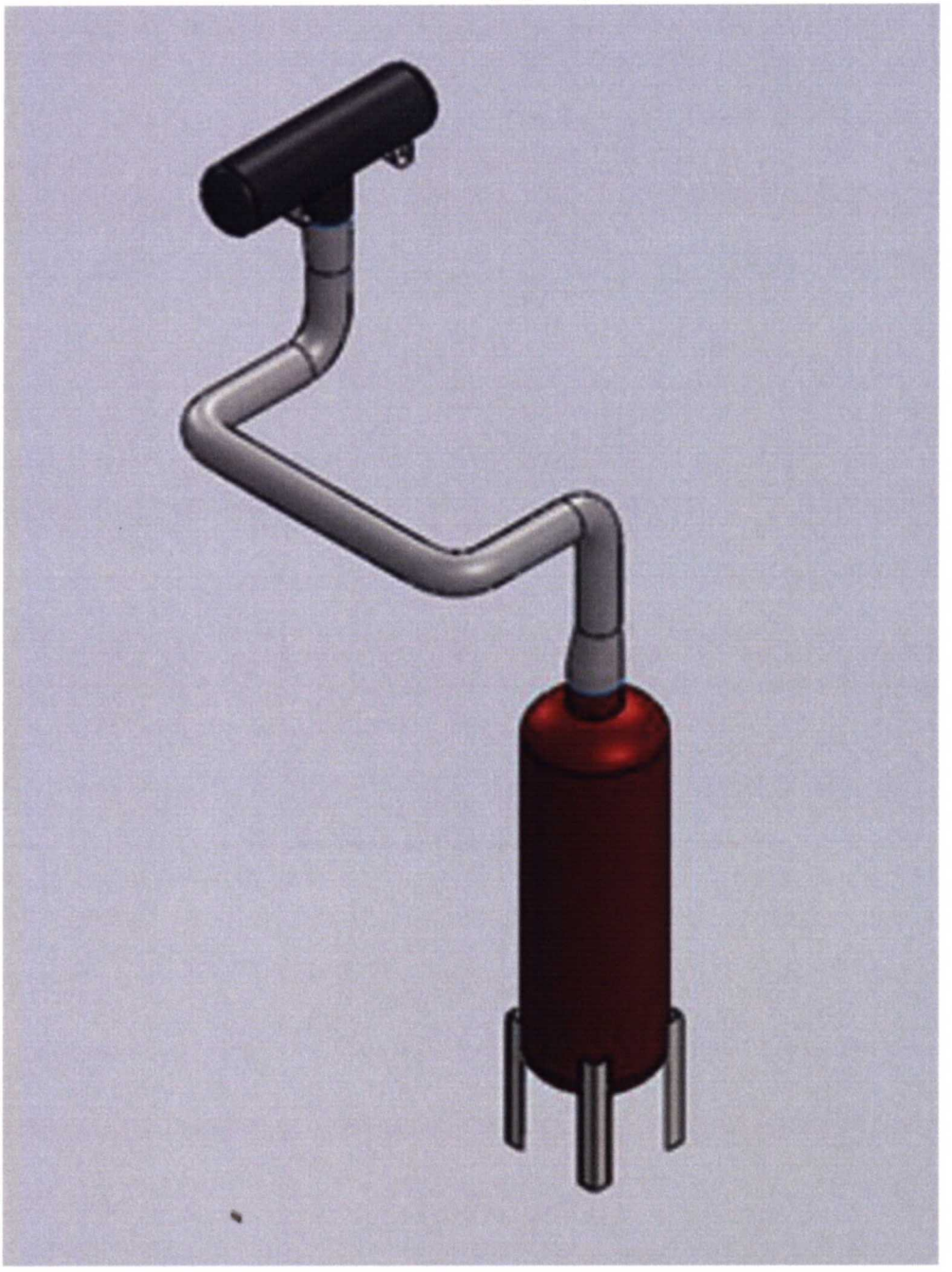

Figure 18: Overall SolidWorks model of the system with flexible nozzle

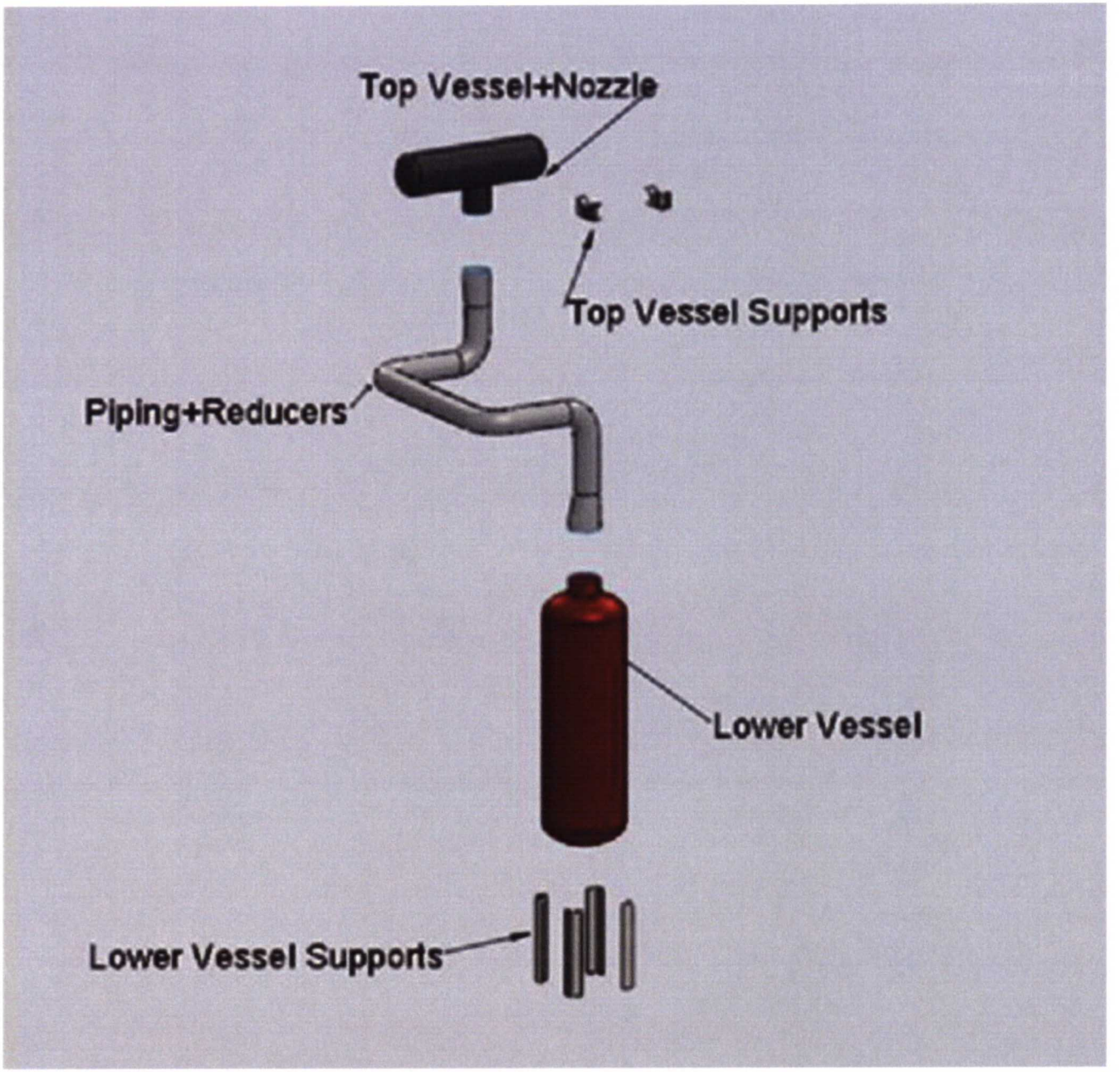

Figure 19: SolidWorks Exploded View of the Piping Model

Appendix D: Nozzle Flexibility Calculations

Calculation of the flexibility factors had been based on (Mershon;Mokhtarian;Ranjan;& Rodabaugh, 1987, ss. 69-71)guidelines and the outcome is the dimensionless quantity representing the ratio of the rotation per unit length of the part in question produced by a moment, to the rotation per unit length of a straight pipe of the same nominal size and schedule or weight produced by the same moment. Three types of flexibility factors had been calculated, such as axial translational, circumferential and longitudinal rotational. Flexibility factors had been calculated using obtained reactions, deflections and rotations at nozzle to shell junctions obtained from CAEpipe and SolidWorks software.

D.1. Design maximum load

Axial translational flexibility is found by

$$\alpha = \left(\frac{P}{w}\right) / \left(\frac{P}{w}\right) PT.LOAD$$

$(P/w)_{PT.LOAD} = 4{,}95ET^2/D\Lambda^{1/2}$

α = stiffness factor;

E=Young's modulus, MPa;

P = radial nozzle load, taken from the CAEpipe or SolidWorks, N;

w= radial deflection due to P, mm;

Nozzle 1 (top nozzle), node 60:

Based on WRC results:

$\Lambda = L / (DT)^{1/2} = 977{,}17 \text{ mm}/(559 \text{ mm} \cdot 12{,}7 \text{ mm})^{1/2} = 977{,}17/84{,}26 = 11{,}6$

$(P/w)_{PT.LOAD} = 4{,}95 \cdot ET^2/D\Lambda^{1/2} = (4{,}95 \cdot 194745 \cdot 9{,}5^2) / (559 \cdot 11{,}6^{1/2}) = 86999894{,}44/1903{,}89 = 45695{,}86;$

P = 14066 N;

w = -0,999 mm (According to CAEpipe results, global displacement in z direction);

$$\alpha = \frac{\left(\frac{14066\ N}{-0{,}999\ mm}\right)}{45695{,}86} = 0{,}31$$

Based on SolidWorks results:

P = -11,17 N;

w = -0,042 mm (According to SolidWorks results, global displacement in y direction, average value of the junction. Root mean square function had not been taken due to the direction-dependent character of the result);

$$\alpha = \frac{\left(\frac{-11{,}17\ N}{-0{,}042\ mm}\right)}{45695{,}86} = 0{,}0058$$

Circumferential rotational flexibility:

Nozzle 1, node 60:

According to CAEpipe results

$$\alpha = \frac{M_{circumferential}}{ET^3\theta} = \frac{-1828000\ N{\cdot}mm}{194745\ \text{MPa}{\cdot}(9{,}5\ mm)^3{\cdot}(-0{,}0032\ rad)} = 3{,}45$$

According to SolidWorks results

$$\alpha = \frac{M_{circumferential}}{ET^3\theta} = \frac{158\ Nmm}{194745\ \text{MPa}{\cdot}9{,}5\ mm^3{\cdot}(-0{,}000047\ rad)} = 0{,}02$$

Circumferential rotational flexibility:

Nozzle 1, node 60:

CAEpipe results:

$$\alpha = \frac{M_{longitudinal}}{ET^3\theta} = \frac{6004000\ Nmm}{194745\ \text{MPa}{\cdot}(9{,}5\ mm)^3{\cdot}(0{,}00085\ rad)} = 42{,}3$$

(According to CAEpipe data for displacement and rotation)

SolidWorks results:

$$\alpha = \frac{M_{longitudinal}}{ET^3\theta} = \frac{17{,}7\ Nmm}{194745\ \text{MPa}{\cdot}(9{,}5\ mm)^3{\cdot}(-0{,}000012\ rad)} = 0{,}0088$$

Nozzle 2, node 10,

Axial translational flexibility:

$(P/w)_{PT.LOAD} = 4{,}95{\cdot}ET^2/D\Lambda^{1/2} = (4{,}95{\cdot}194745{\cdot}12^2) / (880{\cdot}40{,}87^{1/2}) = 138814236/5625{,}81 = 24674{,}54$

CAEpipe results:

P = -23374 N;

w = 9,998 mm;

$$\alpha = \left|\frac{\left(\frac{-23374\ N}{9{,}99\ mm}\right)}{24674{,}54}\right| = 0{,}095$$

The absolute value is taken because of the dimensionless form of the flexibility factor

SolidWorks results:

P = 27,05 N;

w = 0,16 mm (According to CAEpipe results, global displacement in z direction);

$$\alpha = \left|\frac{\left(\frac{27{,}05\ N}{0{,}16\ mm}\right)}{24674{,}54}\right| = 0{,}0069$$

Circumferential rotational flexibility

Nozzle 2, node 10:

CAEpipe results:

$$\alpha = \frac{M_{circumferential}}{ET^3\theta} = \frac{3455000\ Nmm}{194745\ MPa\cdot(12mm)^3\cdot(0{,}0034\ rad)} = 3{,}02$$

SolidWorks results:

$$\alpha = \frac{M_{circumferential}}{ET^3\theta} = \frac{-15{,}2\ Nmm}{194745\ MPa\cdot(12mm)^3\cdot(-0{,}000011\ rad)} = 0{,}0041$$

Longitudinal rotational flexibility

Nozzle 2, node 10:

CAEpipe results:

$$\alpha = \frac{M_{longitudinal}}{ET^3\theta} = \frac{9972000\ Nmm}{194745\ MPa\cdot(12\ mm)^3\cdot(0{,}00098\ rad)} = 30{,}24$$

SolidWorks results:

$$\alpha = \frac{M_{longitudinal}}{ET^3\theta} = \frac{-6{,}2\ Nmm}{194745\ MPa\cdot(12mm)^3\cdot(0{,}0000093\ rad)} = 0{,}002$$

D.2. Operating load

Axial translational flexibility

$(P/w)_{PT.LOAD}=4,95\cdot ET^2/D\Lambda^{1/2}=(4,95\cdot 210367\cdot 9,5^2)/(559\cdot 11,6^{1/2})=93978827,66/1903,89=49361,5$;

Nozzle 1, axial load, node 60:

CAEpipe results:

P = -2305 N;

w = 0 mm;

$$\alpha = rigid$$

SolidWorks results

P = -10,99 N;

w = -0,027 mm;

$$\alpha = \left|\frac{\left(\frac{-10,99\ N}{-0,027mm}\right)}{49361,5}\right| = 0,0082$$

Circumferential rotational flexibility

Nozzle 1, node 60:

CAEpipe results:

$$\alpha = \frac{M_{circumferential}}{ET^3\theta} = \frac{133000\ Nmm}{210367\ \text{MPa}\cdot(9,5\ mm^3)\cdot(0,00023\ rad)} = 3,2$$

SolidWorks results:

$$\alpha = \frac{M_{circumferential}}{ET^3\theta} = \frac{159\ Nmm}{210367\ \text{MPa}\cdot(9,5\ mm^3)\cdot(-0,000017\ rad)} = 0,052$$

Longitudinal rotational flexibility

Nozzle 1, node 60:

CAEpipe results:

$$\alpha = \frac{M_{longitudinal}}{ET^3\theta} = \frac{735000\ Nmm}{210367\ \text{MPa}\cdot(9,5\ mm)^3\cdot(0,0001\ rad)} = 40,75$$

SolidWorks results:

$$\alpha = \frac{M_{longitudinal}}{ET^3\theta} = \frac{17{,}9\ Nmm}{210367\ \text{MPa}\cdot(9{,}5mm)^3\cdot(-0{,}00001\ rad)} = 0{,}01$$

Axial translational flexibility

Nozzle 2, node 10

$(P/w)_{PT.LOAD} = 4{,}95\cdot ET^2/D\Lambda^{1/2} = (4{,}95\cdot 210367\cdot 12^2) / (880\cdot 40{,}87^{1/2}) = 149949598/5625{,}81 = 26654$

CAEpipe results:

P = -7003 N;

w = 1 mm;

$$\alpha = \left|\frac{\left(\frac{-7003\ N}{1\ mm}\right)}{26654}\right| = 0{,}26$$

SolidWorks results:

$$\alpha = \left|\frac{\left(\frac{27{,}04\ N}{-0{,}027\ mm}\right)}{26654}\right| = 0{,}038$$

Circumferential rotational flexibility

Nozzle 2, node 10:

CAEpipe results:

$$\alpha = \frac{M_{circumferential}}{ET^3\theta} = \frac{795000\ Nmm}{210367\cdot 12^3\cdot(0{,}00079\ rad)} = 2{,}77$$

SolidWorks results:

$$\alpha = \frac{M_{circumferential}}{ET^3\theta} = \frac{-14{,}9\ Nmm}{210367\cdot 12^3\cdot(0{,}0000026\ rad)} = 0{,}016$$

Longitudinal rotational flexibility:

Nozzle 2, node 10

CAEpipe results:

$$\alpha = \frac{M_{longitudinal}}{ET^3\theta} = \frac{1432000\ Nmm}{210367 \cdot 12^3 \cdot (0{,}00014\ rad)} = 28{,}14$$

SolidWorks results:

$$\alpha = \frac{M_{longitudinal}}{ET^3\theta} = \frac{-6{,}3\ Nmm}{210367 \cdot 12^3 \cdot (-0{,}0000031\ rad)} = 0{,}0056$$

D.3. Minimum design load

Axial translational load

Nozzle 1, node 60

$(P/w)_{PT.LOAD} = 4{,}95 \cdot ET^2/D\Lambda^{1/2} = (4{,}95 \cdot 213343 \cdot 9{,}5^2) / (559 \cdot 11{,}6^{1/2}) = 95308318{,}5/1903{,}89 = 50060$;

CAEpipe results:

P = -5542 N;

w = 0 mm;

$$\alpha = rigid$$

SolidWorks results:

P = -188,65 N;

w = -0,12 mm;

$$\alpha = \left| \frac{\left(\frac{-188{,}65\ N}{-0{,}12\ mm}\right)}{50060} \right| = 0{,}031$$

Circumferential rotational flexibility

Nozzle 1, node 60:

CAEpipe results:

$$\alpha = \frac{M_{circumferential}}{ET^3\theta} = \frac{501000\ Nmm}{213343 \cdot 9{,}5^3 \cdot (0{,}00087\ rad)} = 3{,}14$$

SolidWorks results:

$$\alpha = \frac{M_{circumferential}}{ET^3\theta} = \frac{2730 Nmm}{213343 \cdot 9{,}5^3 \cdot (-0{,}000038\ rad)} = 0{,}39$$

Longitudinal rotational flexibility

Nozzle 1, node 60:

CAEpipe results:

$$\alpha = \frac{M_{longitudinal}}{ET^3\theta} = \frac{-303000\ Nmm}{213343 \cdot 9{,}5^3 \cdot (-0{,}00004\ rad)} = 41{,}41$$

SolidWorks results:

$$\alpha = \frac{M_{longitudinal}}{ET^3\theta} = \frac{303{,}5\ Nmm}{213343 \cdot 9{,}5^3 \cdot (-0{,}000066\ rad)} = 0{,}025$$

Axial translational flexibility

Nozzle 2, node 10:

$(P/w)_{PT.LOAD} = 4{,}95 \cdot ET^2/D\Lambda^{1/2} = (4{,}95 \cdot 213343 \cdot 12^2) / (880 \cdot 40{,}87^{1/2}) = 152070890{,}4/5625{,}81 = 27031$

CAEpipe results:

P = -3766 N;

w = -1 mm;

$$\alpha = \left|\frac{\left(\frac{-3766\ N}{-1}\right)}{27031}\right| = 0{,}14$$

SolidWorks results:

$$\alpha = \left|\frac{\left(\frac{465{,}17\ N}{-2{,}85}\right)}{27031}\right| = 0{,}006$$

Circumferential rotational flexibility

Nozzle 2, node 10

CAEpipe results:

$$\alpha = \frac{M_{circumferential}}{ET^3\theta} = \frac{295000\ Nmm}{213343 \cdot 12^3 \cdot (0{,}00029\ rad)} = 2{,}76$$

SolidWorks results:

$$\alpha = \frac{M_{circumferential}}{ET^3\theta} = \frac{-259\ Nmm}{213343 \cdot 12^3 \cdot (0{,}00015\ rad)} = 0{,}0047$$

Longitudinal rotational flexibility

Nozzle 2, node 10

CAEpipe results:

$$\alpha = \frac{M_{longitudinal}}{ET^3\theta} = \frac{-250000\ Nmm}{213343 \cdot 12^3 \cdot (-0{,}00002\ rad)} = 33{,}91$$

SolidWorks results:

$$\alpha = \frac{M_{longitudinal}}{ET^3\theta} = \frac{-109 Nmm}{213343 \cdot 12^3 \cdot (-0{,}00014\ rad)} = 0{,}0021$$

Determining the stiffness factor α for the axial nozzle load according to (Mershon;Mokhtarian;Ranjan;& Rodabaugh, 1987, ss. 62-63).

t≥T for both nozzles, therefore the table in mentioned report is valid for both nozzles.

Nozzle 1, node 60

λ = 4,88

Λ = 11,6

According to interpolation, α = 1,37

Nozzle 2, node 10

λ = 3,95

Λ = 40,87

According to interpolation, α = 1,17

D.4. Calculation for the fixed flange assumption

D.4.1. Design maximum load

Axial translational flexibility

Nozzle 1, node 60

$(P/w)_{PT.LOAD} = 4{,}95 \cdot ET^2/D\Lambda^{1/2} = (4{,}95 \cdot 194745 \cdot 9{,}5^2) / (559 \cdot 11{,}6^{1/2}) = 86999894{,}44/1903{,}89 = 45695{,}86$

Based on SolidWorks results:

P = -11,16 N;

w = -0,014 mm (According to SolidWorks results, global displacement in y direction, average value of the junction. Root mean square function had not been taken due to the direction-dependent character of the result);

$$\alpha = \frac{\left(\frac{-11{,}16\ N}{-0{,}014\ mm}\right)}{45695{,}86} = 0{,}017$$

Circumferential rotational flexibility

Nozzle 1, node 60

According to SolidWorks results

$$\alpha = \frac{M_{circumferential}}{ET^3\theta} = \frac{158{,}5\ Nmm}{194745\ \text{MPa}\cdot 9{,}5\ mm^3\cdot(-0{,}0000021\ rad)} = 0{,}45$$

Longitudinal rotational flexibility

Nozzle 1, node 60

SolidWorks results:

$$\alpha = \frac{M_{longitudinal}}{ET^3\theta} = \frac{17{,}7\ Nmm}{194745\ \text{MPa}\cdot(9{,}5\ mm)^3\cdot(-0{,}00003\ rad)} = 0{,}0035$$

Axial translational flexibility

Nozzle 2, node 10

$(P/w)_{PT.LOAD} = 4{,}95\cdot ET^2/D\Lambda^{1/2} = (4{,}95\cdot 194745\cdot 12^2) / (880\cdot 40{,}87^{1/2}) = 138814236/5625{,}809 = 24674{,}54$

SolidWorks results:

P = 27,07 N;

w = 0,013 mm;

$$\alpha = \left|\frac{\left(\frac{27{,}07\ N}{0{,}013\ mm}\right)}{24674{,}54}\right| = 0{,}084$$

Circumferential rotational flexibility

Nozzle 2, node 10

SolidWorks results

$$\alpha = \frac{M_{circumferential}}{ET^3\theta} = \frac{-15{,}2\ Nmm}{194745\ MPa\cdot(12mm)^3\cdot(-0{,}00000095\ rad)} = 0{,}048$$

Longitudinal rotational flexibility

Nozzle 2, node 10:

SolidWorks results:

$$\alpha = \frac{M_{longitudinal}}{ET^3\theta} = \frac{-6{,}12\ Nmm}{194745\ MPa\cdot(12mm)^3\cdot(0{,}0000017\ rad)} = 0{,}011$$

D.4.2. Operating load

Axial translational flexibility

Nozzle 1, node 60

$(P/w)_{PT.LOAD} = 4{,}95\cdot ET^2/D\Lambda^{1/2} = (4{,}95\cdot 210367\cdot 9{,}5^2) / (559\cdot 11{,}6^{1/2}) = 93978827{,}66/1903{,}89 = 49361{,}5$

SolidWorks results

P = -11,01 N;

w = -0,016 mm;

$$\alpha = \left|\frac{\left(\frac{-11{,}01\ N}{-0{,}016\ mm}\right)}{49361{,}5}\right| = 0{,}014$$

Circumferential rotational flexibility

Nozzle 1, node 60

SolidWorks results

$$\alpha = \frac{M_{circumferential}}{ET^3\theta} = \frac{159\ Nmm}{210367\ \text{MPa}\cdot(9{,}5\ mm^3)\cdot(-0{,}00000043\ rad)} = 2{,}05$$

Longitudinal rotational flexibility

Nozzle 1, node 60

SolidWorks results

$$\alpha = \frac{M_{longitudinal}}{ET^3\theta} = \frac{17{,}8\ Nmm}{210367\ \text{MPa}\cdot(9{,}5mm)^3\cdot(-0{,}000022\ rad)} = 0{,}0045$$

Axial translational flexibility

Nozzle 2, node 10

$(P/w)_{PT.LOAD} = 4{,}95\cdot ET^2/D\Lambda^{1/2} = (4{,}95\cdot 210367\cdot 12^2) / (880\cdot 40{,}87^{1/2}) = 149949598/5625{,}81 = 26654$

SolidWorks results:

$$\alpha = \left|\frac{\left(\frac{27{,}03\ N}{-0{,}0068\ mm}\right)}{26654}\right| = 0{,}15$$

Circumferential rotational flexibility

Nozzle 2, node 10

SolidWorks results:

$$\alpha = \frac{M_{circumferential}}{ET^3\theta} = \frac{-15\ Nmm}{210367\cdot 12^3\cdot(0{,}00000068\ rad)} = 0{,}061$$

Longitudinal rotational flexibility

Nozzle 2, node 10

SolidWorks results:

$$\alpha = \frac{M_{longitudinal}}{ET^3\theta} = \frac{-6{,}3\ Nmm}{210367\cdot 12^3\cdot(-0{,}0000036\ rad)} = 0{,}005$$

D.4.3. Minimum design load:

Axial translational flexibility

Nozzle 1, node 60

$(P/w)_{PT.LOAD} = 4{,}95\cdot ET^2/D\Lambda^{1/2} = (4{,}95\cdot 213343\cdot 9{,}5^2) / (559\cdot 11{,}6^{1/2}) = 95308318{,}5/1903{,}89 = 50060$

SolidWorks results:

P = -188,65 N;

w = -0,12 mm;

$$\alpha = \left| \frac{\left(\frac{-188{,}65\ N}{-0{,}12\ mm}\right)}{50060} \right| = 0{,}031$$

Circumferential rotational flexibility

Nozzle 1, node 60

SolidWorks results:

$$\alpha = \frac{M_{circumferential}}{ET^3\theta} = \frac{2729Nmm}{213343 \cdot 9{,}5^3 \cdot (-0{,}000039\ rad)} = 0{,}38$$

Longitudinal rotational flexibility

Nozzle 1, node 60

SolidWorks results:

$$\alpha = \frac{M_{longitudinal}}{ET^3\theta} = \frac{303{,}5\ Nmm}{213343 \cdot 9{,}5^3 \cdot (-0{,}000015\ rad)} = 0{,}11$$

Axial translational flexibility

Nozzle 2, node 10,

$(P/w)_{PT.LOAD} = 4.95 \cdot ET^2/D\Lambda^{1/2} = (4.95 \cdot 213343 \cdot 12^2) / (880 \cdot 40{,}87^{1/2}) = 152070890{,}4/5625{,}81 = 27031$

SolidWorks results:

$$\alpha = \left| \frac{\left(\frac{465{,}17\ N}{-2{,}85}\right)}{27031} \right| = 0{,}006$$

Circumferential rotational flexibility

Nozzle 2, node 10

SolidWorks results:

$$\alpha = \frac{M_{circumferential}}{ET^3\theta} = \frac{-258{,}5\ Nmm}{213343 \cdot 12^3 \cdot (0{,}00015\ rad)} = 0{,}0047$$

Longitudinal rotational flexibility

Nozzle 2, node 10

SolidWorks results:

$$\alpha = \frac{M_{longitudinal}}{ET^3\theta} = \frac{-109Nmm}{213343 \cdot 12^3 \cdot (-0{,}00014\,rad)} = 0{,}0021$$

Let us compile the obtained data into the table for comparison:

Flexibility coefficient α												
	Design maximum				Operating				Design minimum			
	CAEpipe	FEM	FEM with fixed flanges	WRC	CAEpipe	FEM	FEM with fixed flanges	WRC	CAEpipe	FEM	FEM with fixed flanges	WRC
P	0,31	0,0058	0,017	1,37	Rigid	0,0082	0,014	1,37	Rigid	0,031	0,031	1,37
M_C	3,45	0,02	0,45	2,9	3,2	0,052	2,05	2,9	3,14	0,39	0,38	2,9
M_L	42,3	0,0088	0,0035	2,16	40,75	0,01	0,0045	2,16	41,41	0,025	0,11	2,16
P	0,095	0,0069	0,084	1,17	0,263	0,038	0,15	1,17	0,14	0,006	0,006	1,17
M_C	3,02	0,0041	0,048	2,6	2,77	0,016	0,061	2,6	2,76	0,0047	0,0047	2,6
M_L	30,24	0,002	0,011	19,4	28,14	0,0056	0,005	19,4	33,91	0,0021	0,0021	19,4

Table 36: Flexibility coefficients comparison

D.5. Comparison of nozzle flexibility factors for different load cases for obtained from FEM simulation results

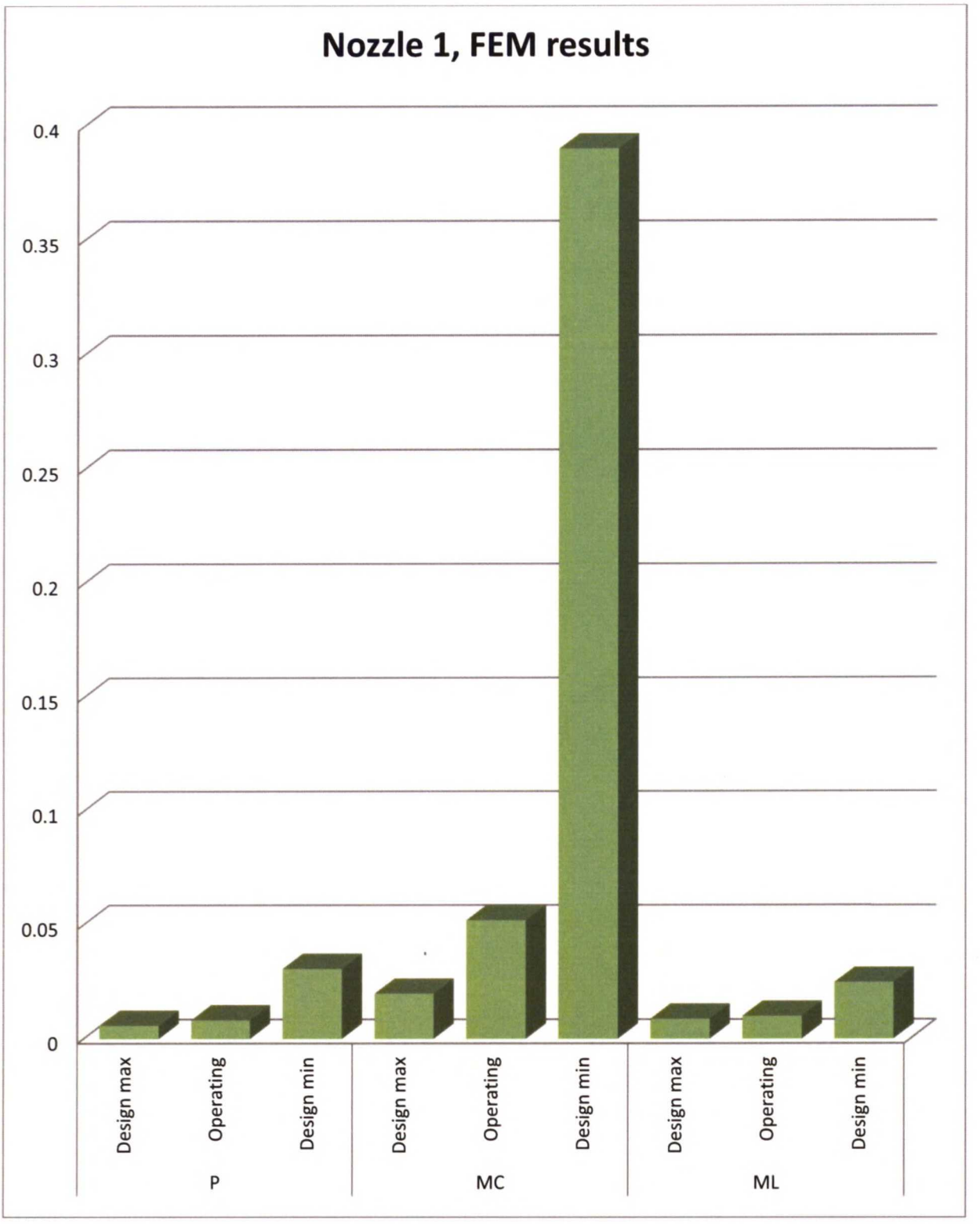

Figure 20: Comparison of nozzle flexibility factors for different load cases for nozzle 1 obtained from FEM simulation

r

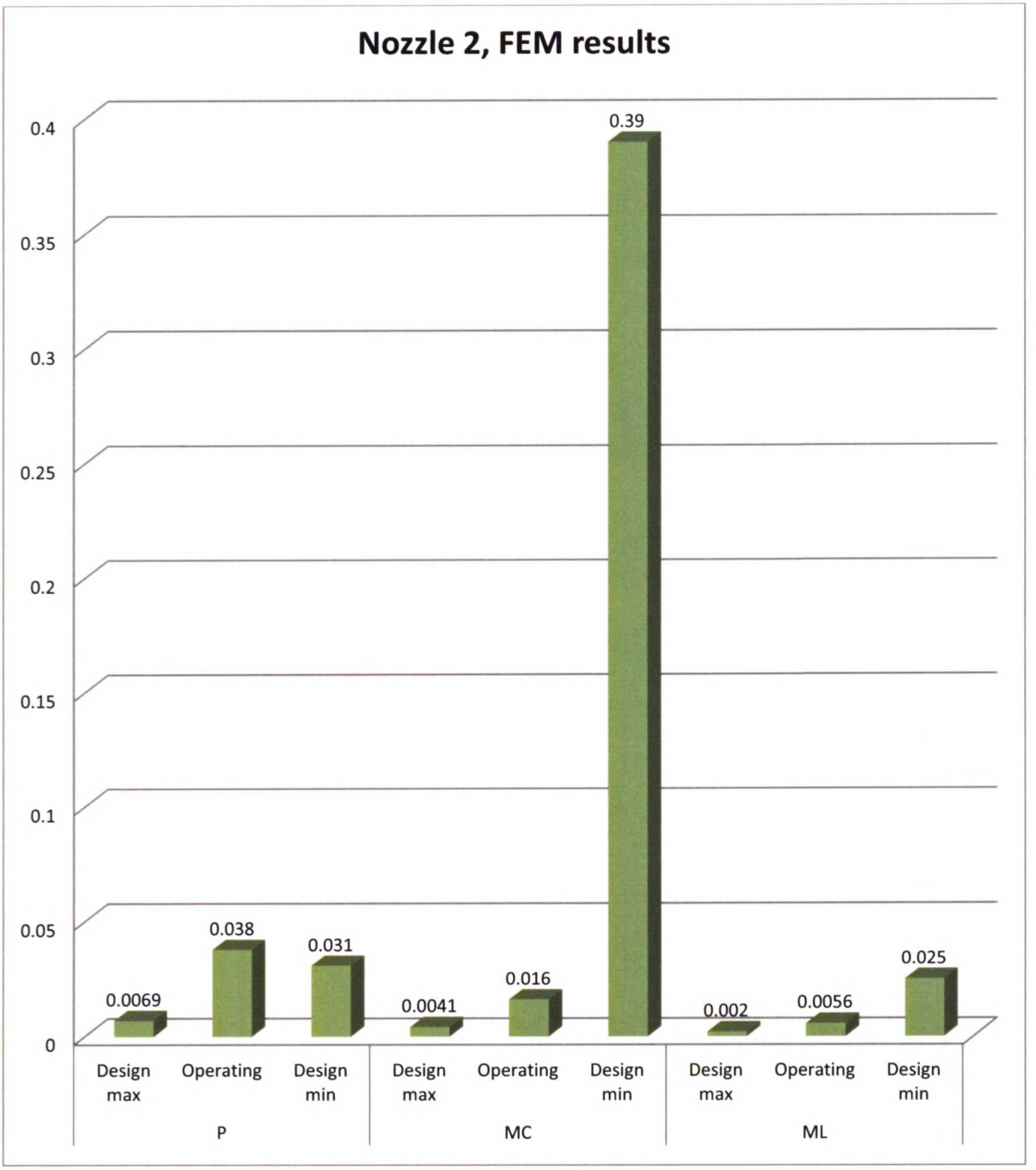

Figure 21: Comparison of nozzle flexibility factors for different load cases for nozzle 2 obtained from FEM simulation

Appendix E: Nozzle load comparison

E.1. Nozzle load comparison

E.1.1. Design maximum load case

E.1.1.1. Nozzle 1

	Axial force, kN	Difference between the allowable and real load, %	Circumferential moment, kNm	Difference between the allowable and real load, %	Longitudinal moment, kNm	Difference between the allowable and real load, %
Allowable load	16,38	-	17,64	-	17,64	-
CAEpipe rigid	17,57	7,3	-8,16	-53,7	14,76	-16,3
CAEpipe flexible	14,07	-14,1	-1,83	-89,6	6,00	-66,0
FEM	0,011	-99,9	-0,0016	-100,0	-0,00018	-100,0

Table 37: Comparison of the reaction loads on nozzle 1, design maximum load.

E.1.1.2.Nozzle 2

	Axial force, kN	Difference between the allowable and real load, %	Circumferential moment, kNm	Difference between the allowable and real load, %	Longitudinal moment, kNm	Difference between the allowable and real load, %
Allowable load	18,72	-	23,04	-	23,04	-
CAEpipe rigid	-26,88	43,6	11,14	-51,7	20,40	-11,5
CAEpipe flexible	-23,37	24,9	3,46	-85,0	9,97	-56,7
FEM	0,027	-100	-0,00015	-100	-0,000062	-100

Table 38: Comparison of the reaction loads on nozzle 2, design maximum load.

E.1.2. Operating load case

E.1.2.1. Nozzle 1

	Axial force, kN	Difference between the allowable and real load, %	Circumferential moment, kNm	Difference between the allowable and real load, %	Longitudinal moment, kNm	Difference between the allowable and real load, %
Allowable load	16,38	-	17,64	-	17,64	-
CAEpipe rigid	-2,15	-86,9	-1,00	-94,3	2,05	-88,4
CAEpipe flexible	-2,31	-85,9	0,13	-99,3	0,74	-95,8
FEM	-0,011	-99,9	0,0016	-100	0,00018	-100

Table 39: Comparison of the reaction loads on nozzle 1, operating load

E.1.2.2.Nozzle 2

	Axial force, kN	Difference between the allowable and real load, %	Circumferential moment, kNm	Difference between the allowable and real load, %	Longitudinal moment, kNm	Difference between the allowable and real load, %
Allowable load	18,72	-	23,04	-	23,04	-
CAEpipe rigid	-7,16	-61,7	2,94	-87,2	2,54	-89,0
CAEpipe flexible	-7,00	-62,6	0,80	-96,5	1,43	-93,8
FEM	0,027	-99,9	-0,00015	-100	-0,000063	-100

Table 40: Comparison of the reaction loads on nozzle 2, operating load

E.1.3. Design minimum load

E.1.3.1. Nozzle 1

	Axial force, kN	Difference between the allowable and real load, %	Circumferential moment, kNm	Difference between the allowable and real load, %	Longitudinal moment, kNm	Difference between the allowable and real load, %
Allowable load	16,38	-	17,64	-	17,64	-
CAEpipe rigid	-5,75	-64,9	-0,37	-97,9	2,67	-84,8
CAEpipe flexible	-5,54	-66,2	0,50	-97,2	0,30	-98,3
FEM	-0,19	-98,8	-0,027	-99,8	-0,003	-100,0

Table 41: Comparison of the reaction loads on nozzle 1, design minimum load.

E.1.3.2. Nozzle 2

	Axial force, kN	Difference between the allowable and real load, %	Circumferential moment, kNm	Difference between the allowable and real load, %	Longitudinal moment, kNm	Difference between the allowable and real load, %
Allowable load	18,72	-	23,04	-	23,04	-
CAEpipe rigid	-3,56	-81,0	-0,83	-96,4	1,45	-93,7
CAEpipe flexible	-3,77	-79,9	0,30	-98,7	-0,25	-98,9
FEM	-0,47	-97,5	-0,0026	-100,0	-0,0011	-100,0

Table 42: Comparison of the reaction loads on nozzle 2, design minimum load

E.2. Comparison of design maximum and operating load

E.2.1. CAEpipe rigid assumption

Nozzle 1, node 60	**Allowable nozzle load**	**Design maximum**	**Operating**
Axial, kN	16,38	17,57	2,15
Circumferential mom, kNm	17,64	8,16	1,00
Longitudinal mom, kNm	17,64	14,76	2,05
Nozzle 2, node 10	**Allowable nozzle load**	**Design maximum**	**Operating**
Axial, kN	18,72	26,88	7,16
Circumferential mom, kNm	23,04	11,14	2,94
Longitudinal mom, kNm	23,04	20,40	2,54

Table 43: Comparison between allowable loads, design maximum load case and operating load case for CAEpipe rigid assumption

E.2.2. CAEpipe flexible assumption

Nozzle 1, node 60	**Allowable nozzle load**	**Design maximum**	**Operating**
Axial, kN	16,38	14,07	2,31
Circumferential mom, kNm	17,64	1,83	0,13
Longitudinal mom, kNm	17,64	6,00	0,74
Nozzle 2, node 10	**Allowable nozzle load**	**Design maximum**	**Operating**
Axial, kN	18,72	23,37	7,0
Circumferential mom, kNm	23,04	3,46	0,8
Longitudinal mom, kNm	23,04	9,97	1,43

Table 44: Comparison between allowable loads, design maximum load case and operating load case for CAEpipe flexible assumption

E.2.3. FEM model

Nozzle 1, node 60	Allowable nozzle load	Design max	Operating
Axial, kN	16,38	-0,011	-0.011
Circumferential mom, kNm	17,64	0,0016	0.0016
Longitudinal mom, kNm	17,64	0,00018	0.00018
Nozzle 2, node 10	**Allowable nozzle load**	**Design max**	**Operating**
Axial, kN	18,72	0,027	0.027
Circumferential mom, kNm	23,04	-0,00015	-0.00015
Longitudinal mom, kNm	23,04	-0,00062	-0.000063

Table 45: Comparison between allowable loads, design maximum load case and operating load case for FEM modelling in SolidWorks environment

Difference of the nozzle load in FEM modelling for the design maximum and operating load case is insignificant, thus the difference in flexibility factor had been observed for different load cases due to the diverse values of the internal pressure. Nevertheless, difference between the exerted displacements is substantial and can be found in Table 46.

20.08.2013. Irina Filatova

Nozzle 1, node 60	Design max	Operating
Axial displacement, mm	-0,014	-0,016
Circumferential rotation, rad	-0,0000021	-0,00000043
Longitudinal rotation, rad	-0,00003	-0,000022
Nozzle 2, node 10	**Design max**	**Operating**
Axial displacement, mm	0,013	-0,0068
Circumferential rotation, rad	-0,00000095	0,00000068
Longitudinal rotation, rad	0,0000017	-0,0000036

Table 46: Comparison of the exerted displacements for FEM modelling between design maximum and operating load cases

Appendix F: Material model

F.1. Material model in CAEpipe 6.81

Pipe material 106: A106 Grade B

Density = 7833 (kg/m3), Nu = 0.300, Joint factor = 1.00, Type = CS
Yield strength = 241.3 (MPa)

Temp (C)	E (MPa)	Alpha (mm/mm/C)	Allowable (MPa)
-28.89	205946	10.55E-6	137.9
37.78	202016	11.03E-6	137.9
93.33	198569	11.48E-6	137.9
148.9	195122	11.88E-6	137.9
204.4	190985	12.28E-6	137.2
260	188227	12.64E-6	131.0
315.6	184090	13.01E-6	123.4
343.3	179953	13.19E-6	119.3
371.1	175816	13.39E-6	115.1
398.9	171335	13.57E-6	95.84

Figure 22: CAEpipe 6.81 Material Model

F.2. Material model in SolidWorks 2012

F.2.1. S355 JR mechanical properties

Temperature, °C	Elastic modulus, MPa
40	210367
250	194745

Table 47: S355 JR Elastic modulus data

Temperature, °C	Yield strength, MPa
21	265
40	265

Table 48: S355 JR Yield strength data

Temperature, °C	Thermal expansion coefficient, mm/mm/°C
-28,89	$1,06 \cdot 10^{-5}$
37,78	$1,10 \cdot 10^{-5}$
93,33	$1,15 \cdot 10^{-5}$
148,9	$1,19 \cdot 10^{-5}$
204,4	$1,23 \cdot 10^{-5}$
260	$1,26 \cdot 10^{-5}$

Table 49: S355 JR Thermal expansion coefficient data

F.2.2. SA106 Grade B mechanical and physical properties

Temperature, °C	Elastic modulus, MPa
-28.89	2059446
37,78	202016
93,33	198569
148,9	195122
204,4	190985
260	188227

Table 50: SA106 Grade B Elastic modulus data

Temperature, °C	Yield strength, MPa
-28,89	153.07
37,78	153.07
93,33	153.07
148,9	153.07
204,4	152.29
260	145.41

Table 51: SA106 Grade B Yield strength data

Temperature, °C	Thermal expansion coefficient, mm/mm/°C
-28,89	$1.06 \cdot 10^{-5}$
37,78	$1.10 \cdot 10^{-5}$
93,33	$1.15 \cdot 10^{-5}$
148,9	$1.19 \cdot 10^{-5}$
204,4	$1.23 \cdot 10^{-5}$
260	$1.26 \cdot 10^{-5}$

Table 52: SA106 Grade B Thermal expansion coefficient data

F.2.3. P275 NH mechanical and physical properties

Temperature, °C	Elastic modulus, MPa
0	213342.6
40	210367
250	194745
285	192141.3

Table 53: P275 NH Elastic modulus data

Temperature, °C	Yield strength, MPa
40	275
50	266
100	250
150	232
200	213
250	195
285	182

Table 54: P275 NH Yield strength data

Temperature, °C	Thermal expansion coefficient, mm/mm/°C
-28,89	$1{,}06 \cdot 10^{-5}$
37,78	$1{,}10 \cdot 10^{-5}$
93,33	$1{,}15 \cdot 10^{-5}$
148,9	$1{,}19 \cdot 10^{-5}$
204,4	$1{,}23 \cdot 10^{-5}$
260	$1{,}26 \cdot 10^{-5}$

Table 55: P275 NH Yield strength data

pendix G: Original Drawings

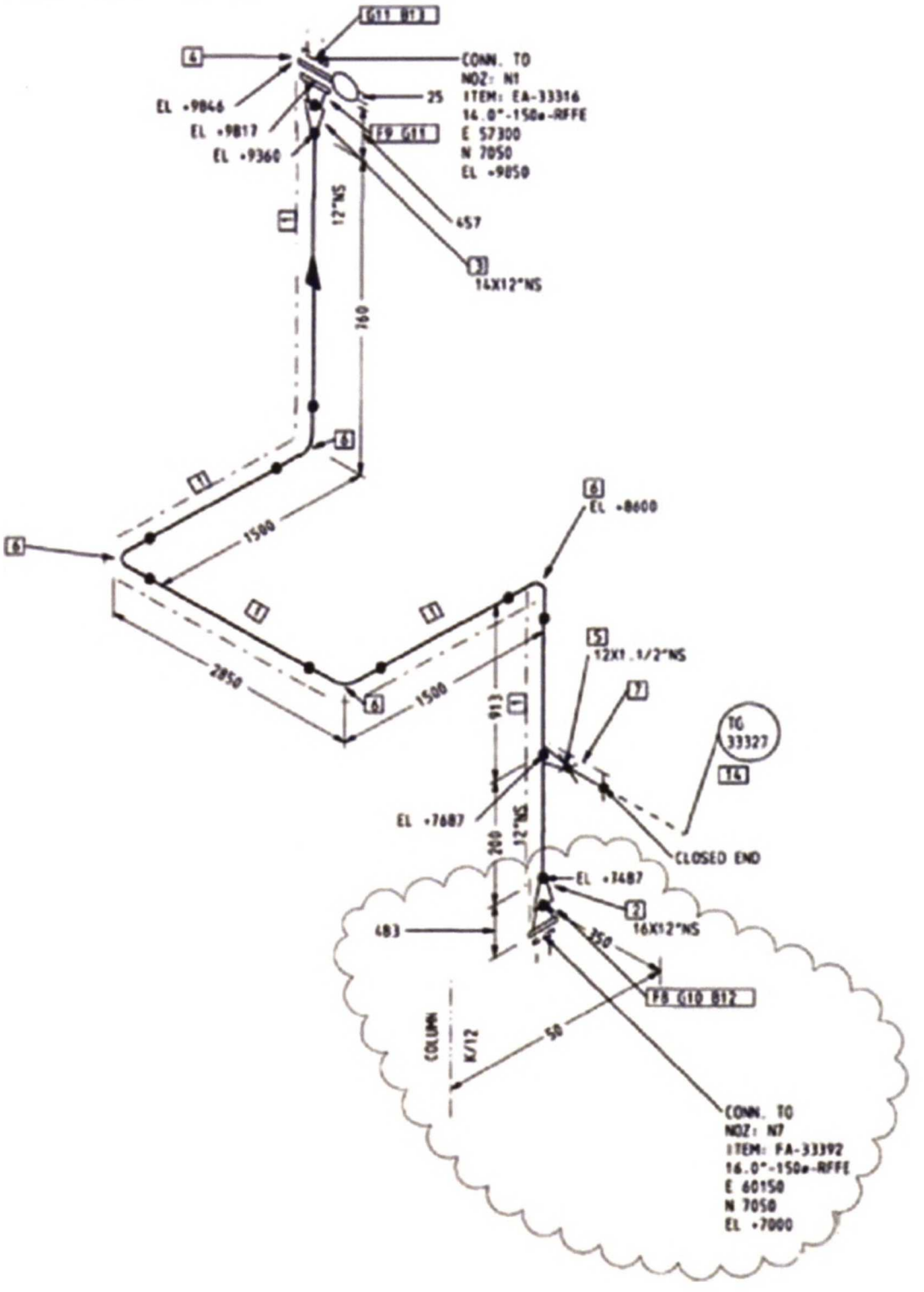

ure 23: Original drawing of the piping isometrics

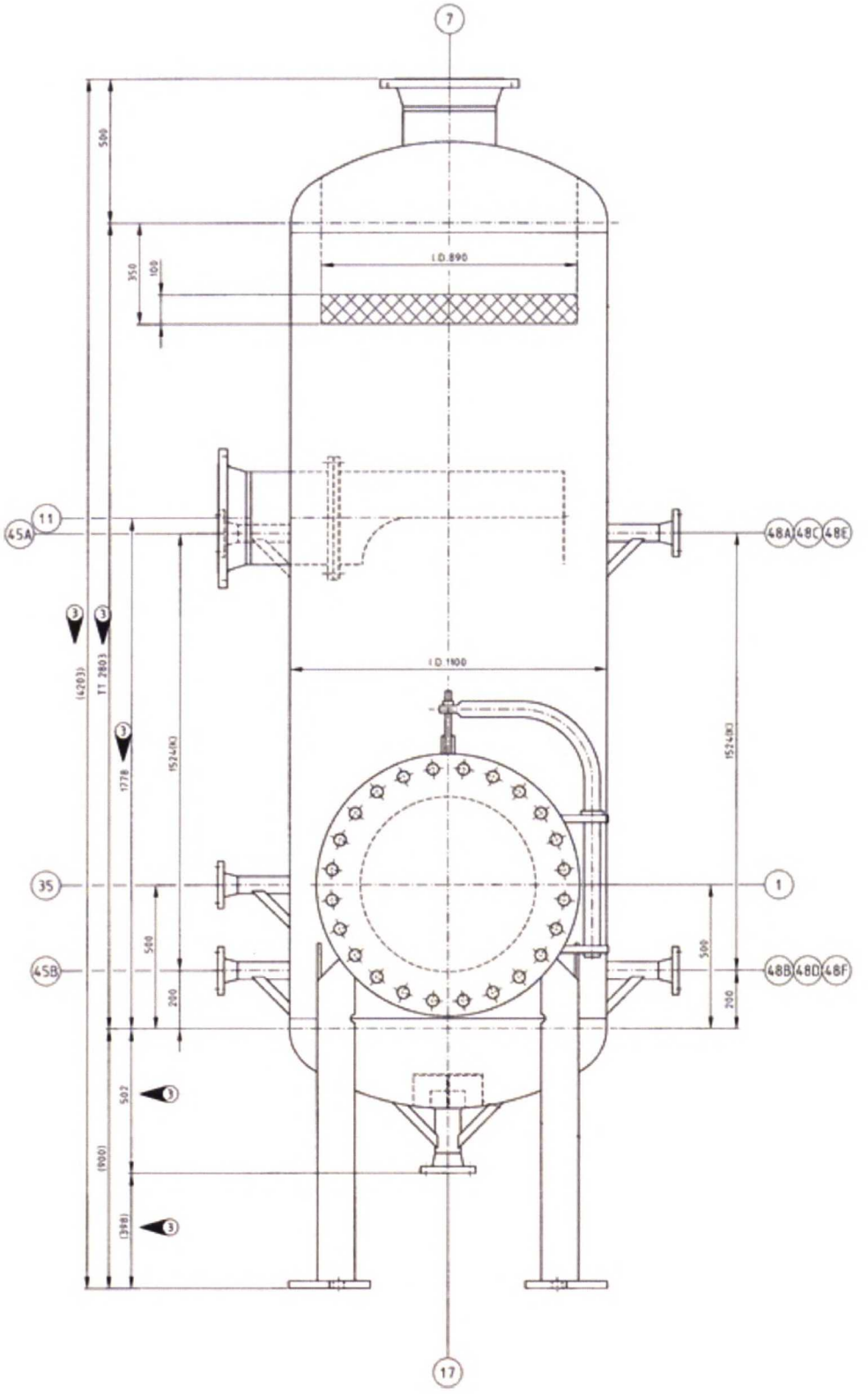

ure 24: Original drawing of the lower vessel

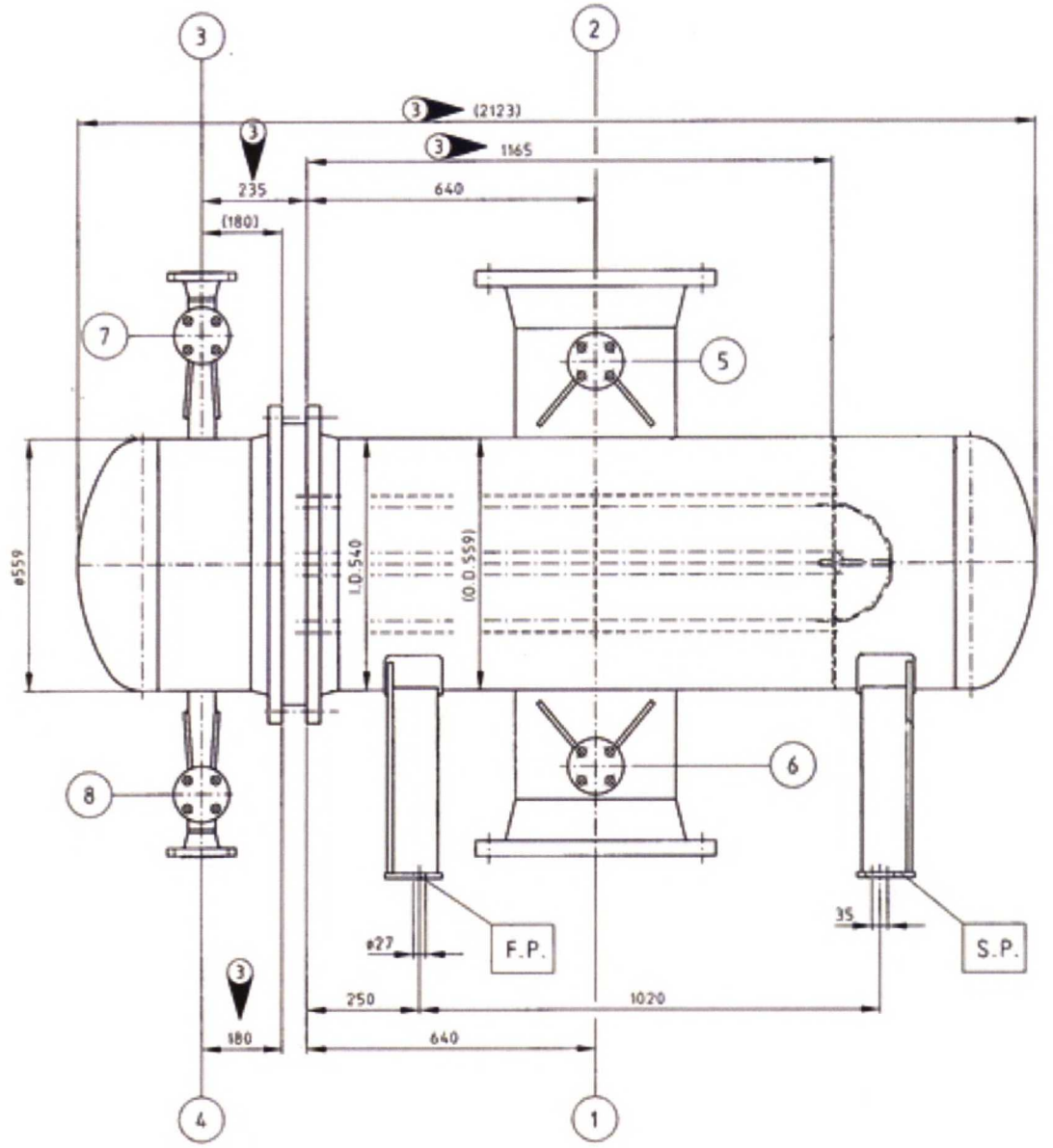

ure 25: Original drawing of the top vessel